STRUCTURE OF ALP CONVERSION AT NEUTRON STARS

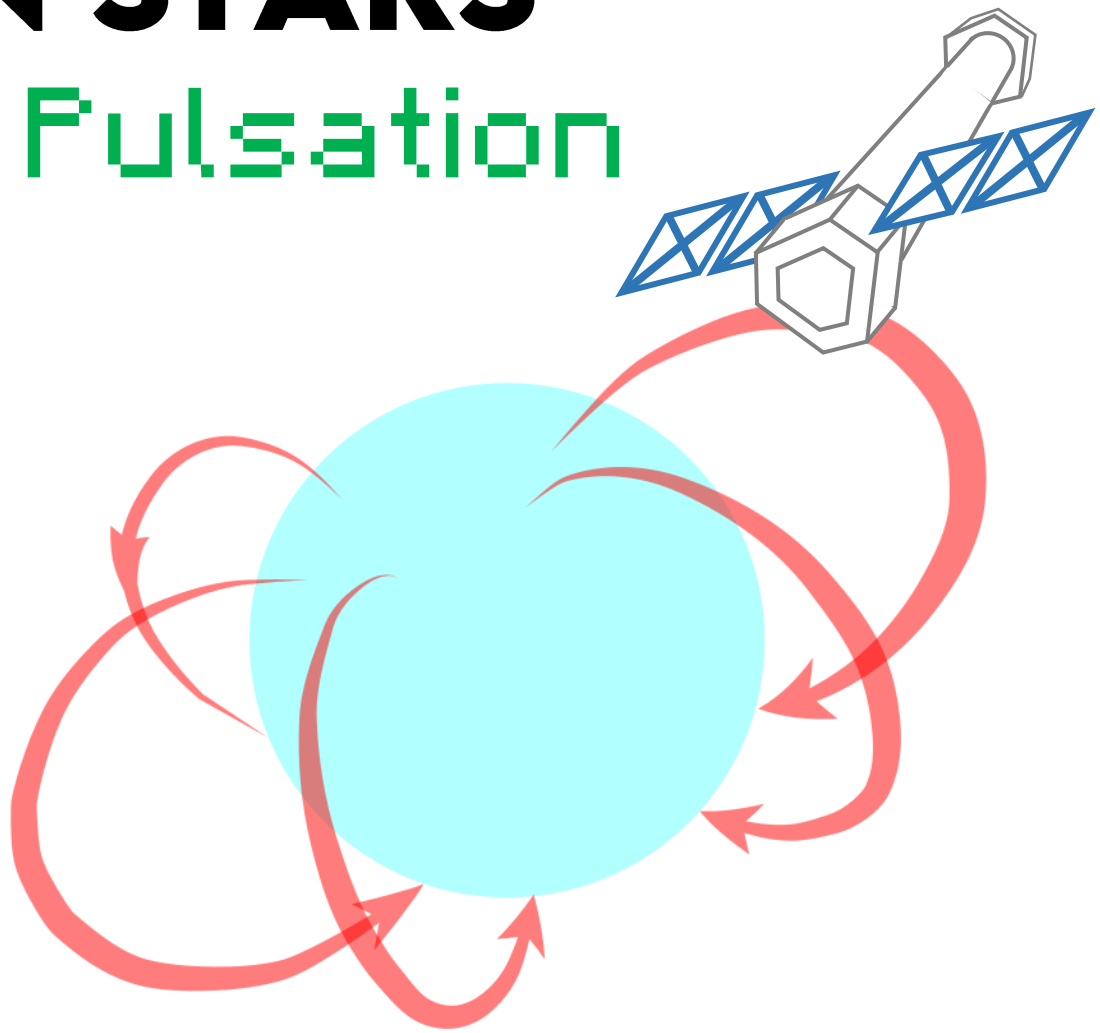
Polarization & Pulsation

Lingfeng Li 李凌风

Sep. 18, 2026, Dali

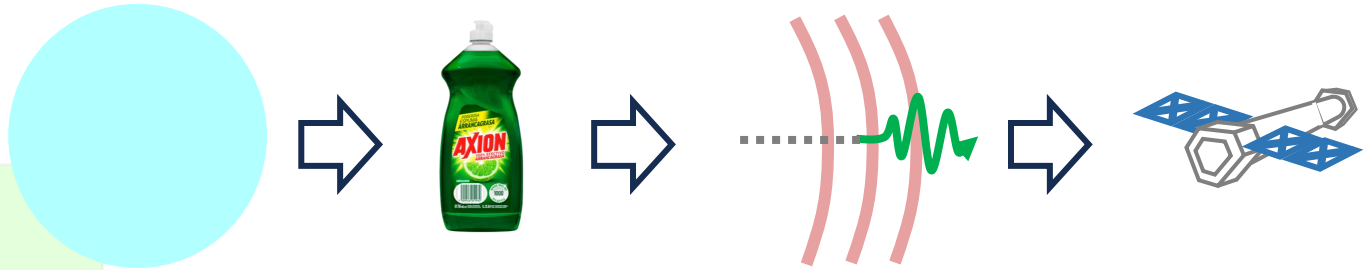
Axion-Photon Conversion:

Terrestrial and Cosmic Searches

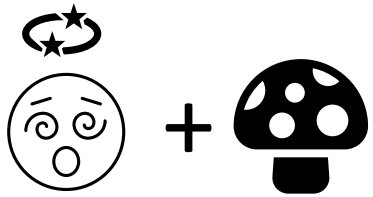


arXiv:2501.12440
JiJi Fan, LFL, Chen Sun
PRL 135 (2025), 231801

Outline



- Introduction: What's a Pulsar (and axion related works)?
- Axion production and conversion to photon in the NS
- NS rotation modulate conversion: pulse and polarization
- A case study of RX J1856.5-3754, one from the "magnificent 7"
- Outlook



Why Neutron Star?

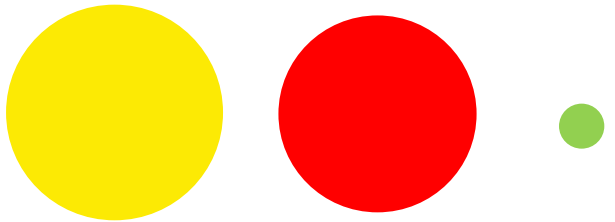


First discussed in public:
Lev Landau, 1932

First observation as radio pulsars in 1967

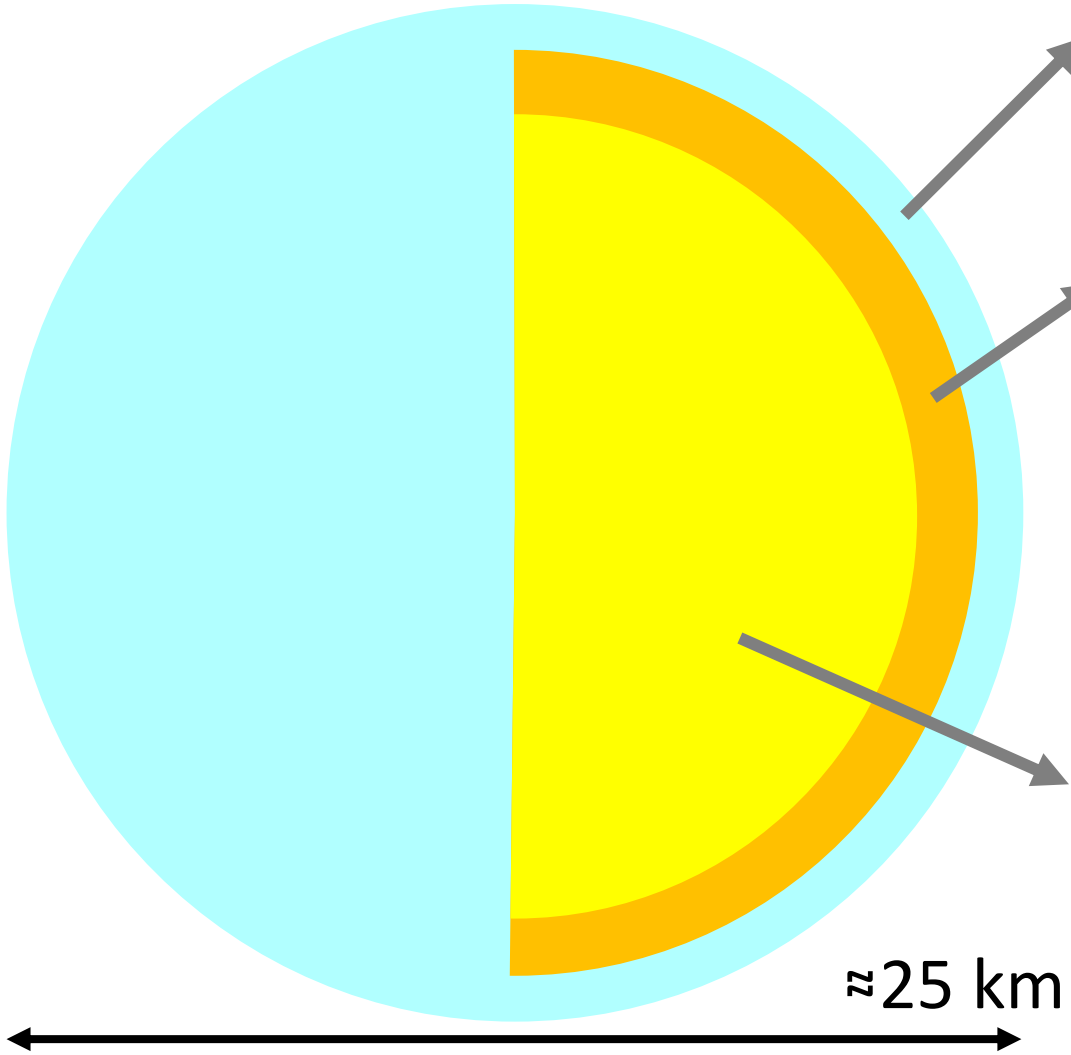
See also: D. G. Yakovlev1, P. Haensel, G. Baym3, C. J. Pethick, 1210.0682

$$m_n > m_p + m_e$$



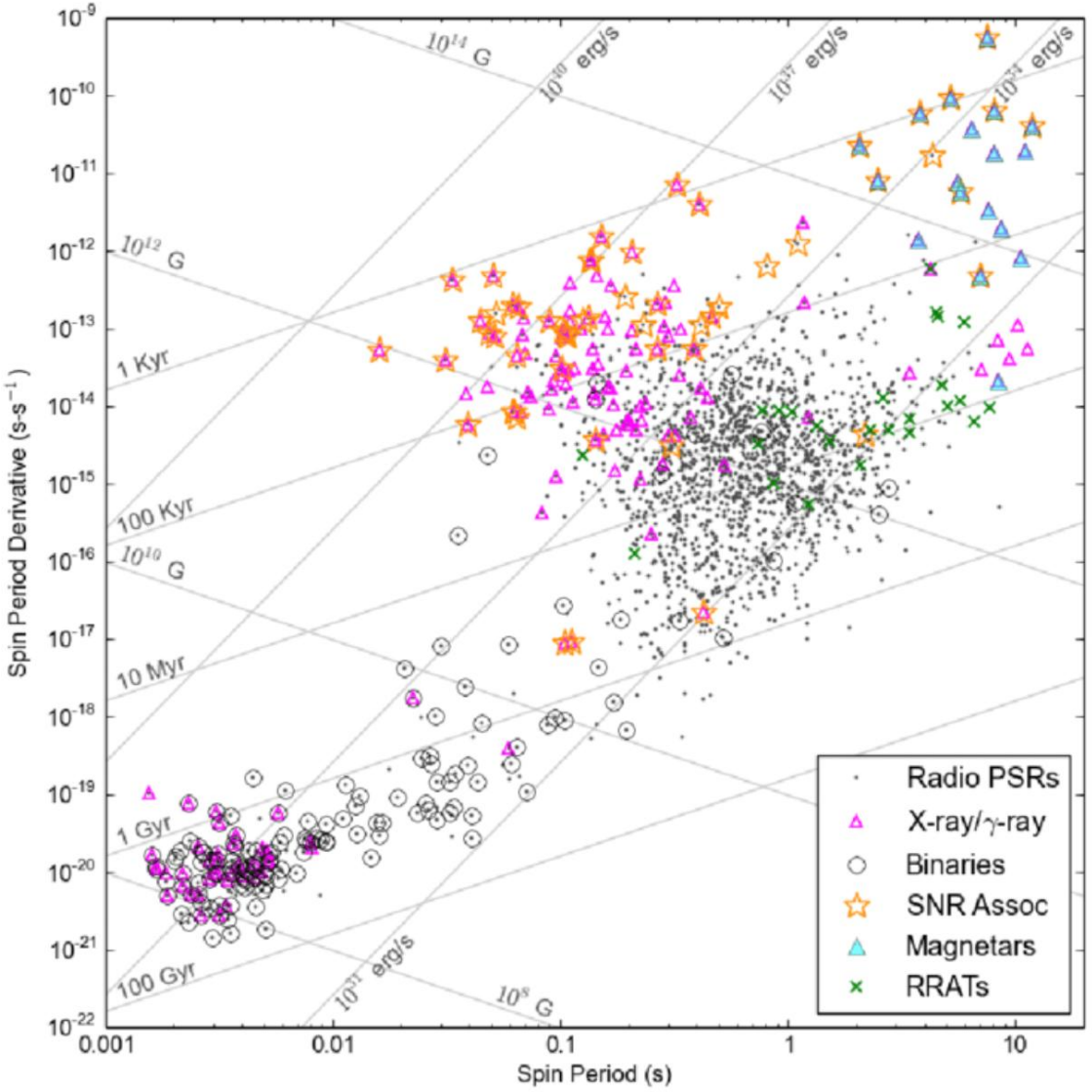
Free neutrons decay, need HUGE pressure to compress electrons and protons →neutrons

Pulsar in a Nutshell



- Gaseous Iron Atmosphere (~cm) thick
- Degenerate Electron State Outer Surface (Fermi pressure provided by electrons)
- Neutron-Rich Core Region with Exotic Matter (Neutron Fermi momentum reaching ~O(100) MeV)

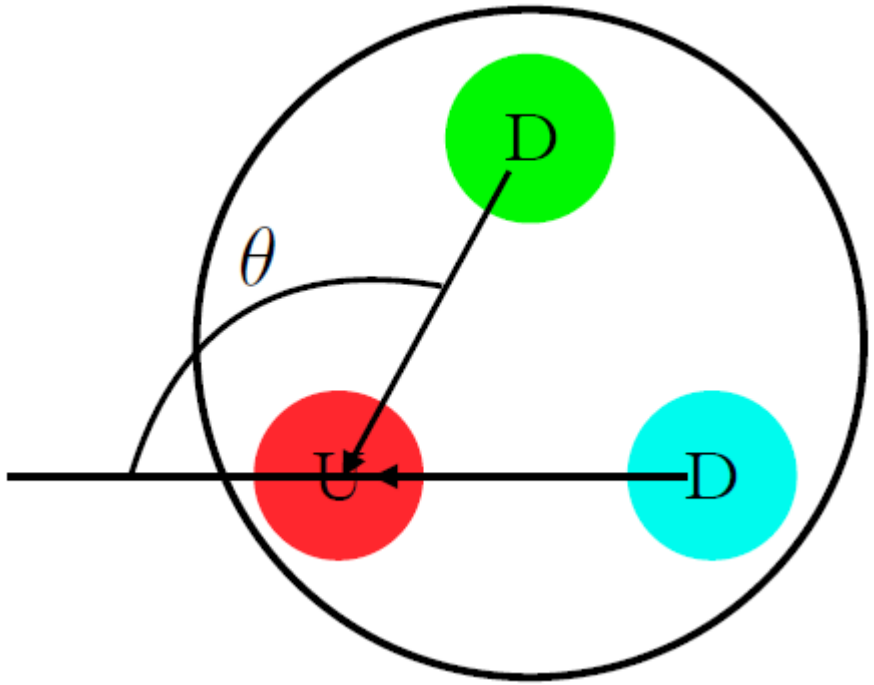
Pulsar in a Nutshell (II)



- Spin period varies from 10s to milliseconds
- VERY strong magnetic field: Critical B field: $\approx 10^{14}$ Gauss $\approx m_e^2$
- Surface feature also varies, leading to different electromagnetic signals
- Core temperature up to O(100) KeV

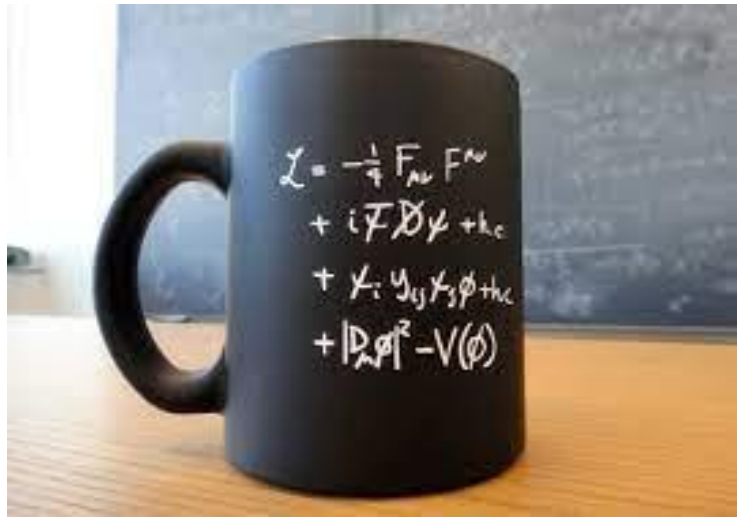
The Strong CP Problem

Allowed in SM, arises from SU(3) topology



A. Hook, 2018

$$\mathcal{L} \supset \theta \frac{g^2}{32\pi^2} G\tilde{G}$$



Experimental hints: neutron EDM

Natural expectation: $O(Q \times fm) \approx 10^{-13}$ e cm

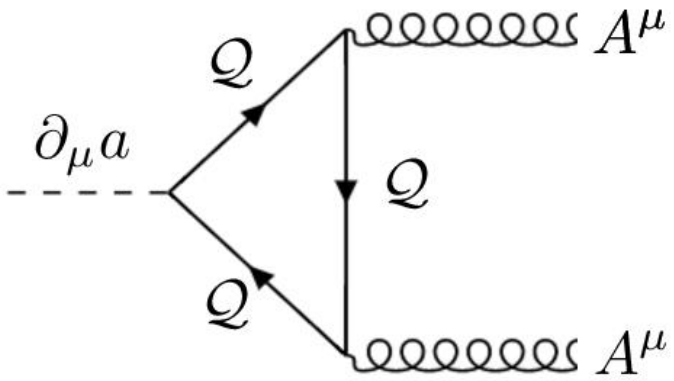
Experimental result $\lesssim 10^{-26}$ e cm, $\theta \lesssim 10^{-10}$

Small dimensionless parameters may not be natural: protected by some mechanism?

PQ Symmetry and QCD Axion

QCD axion: A pseudo Nambu-Goldstone Boson (pNGB) of a the Peccei-Quinn symmetry

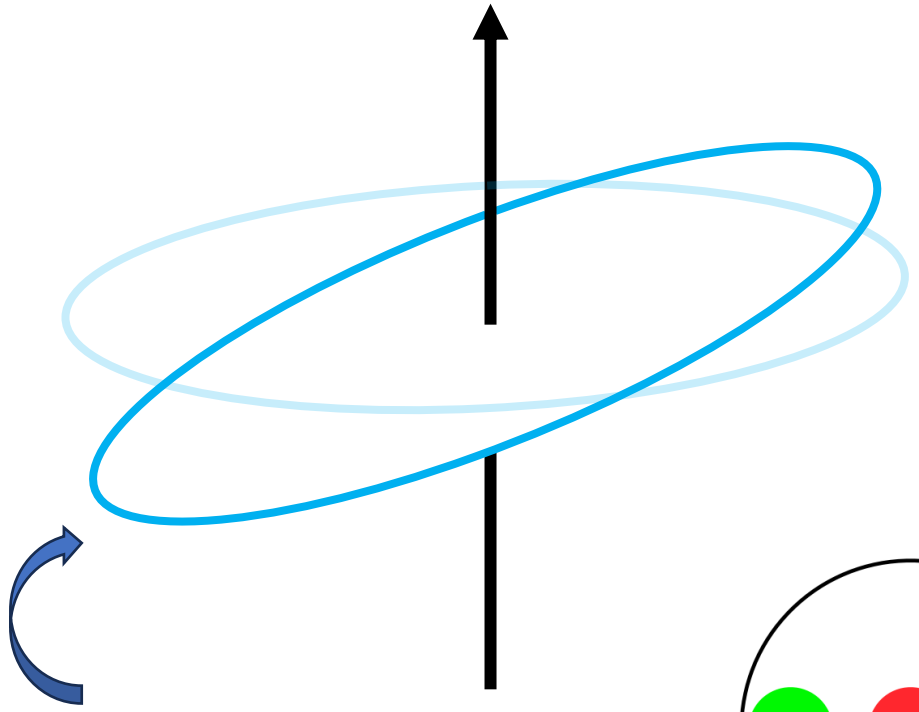


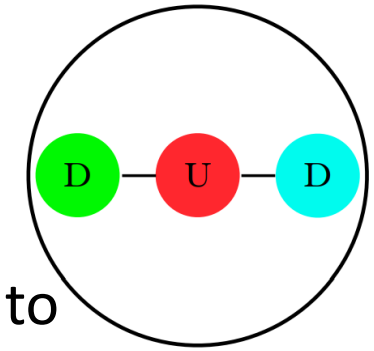


$$\mathcal{L} \supset \left(\frac{a}{f_a} + \theta\right) \frac{1}{32\pi^2} G\tilde{G}$$

Greater than ~10^9 GeV from data

$$V = -m_\pi^2 f_\pi^2 \sqrt{1 - \frac{4 m_u m_d}{(m_u + m_d)^2} \sin^2\left(\frac{a}{2f_a} + \frac{\bar{\theta}}{2}\right)}$$





The strong CP θ angle are set to zero at the minima during the current universe

Peccei, Quinn; Weinberg; Wilczek; Kim; Shifman, Vainshtein, Zakharov; Zhitnitsky; Dine, Fischler, Srednicki, 1977-1981

The axion-like particle (ALP)

- Motivated by other theories in the UV (e.g. the string axiverse picture)

EFT coupling with the photon field

$$\mathcal{L} \supset \frac{g_{a\gamma}}{4} a F^{\mu\nu} \tilde{F}_{\mu\nu}$$

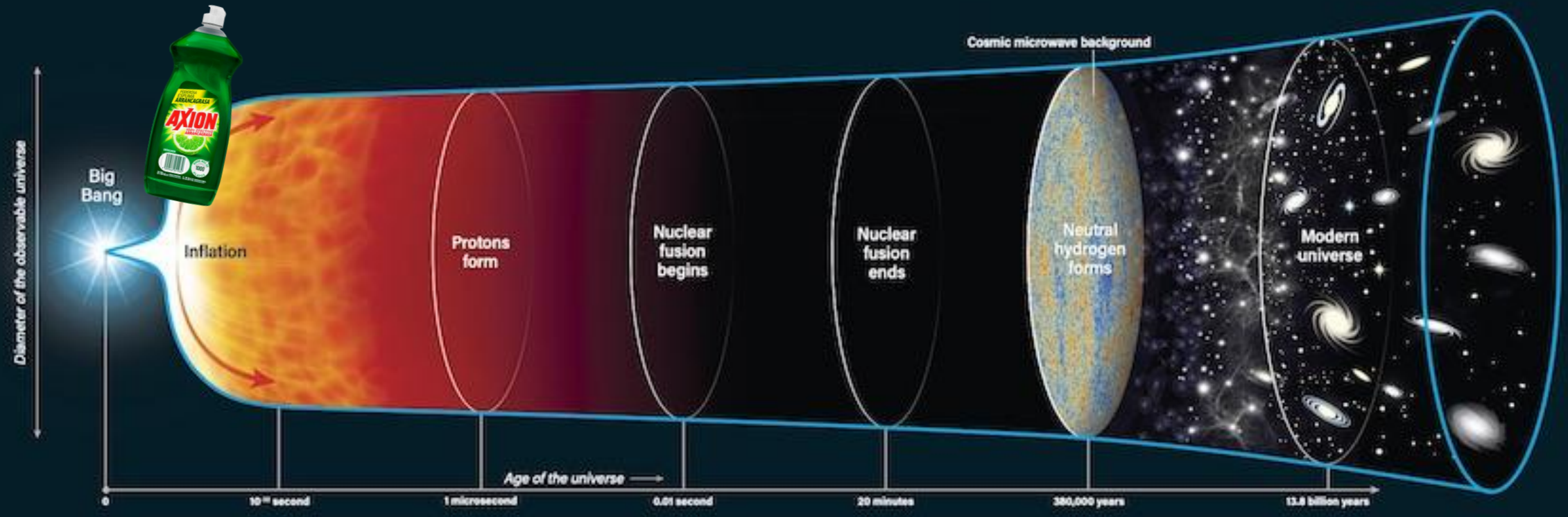
$$\frac{g_{af}\,\partial^{\mu} a}{2m_f} \bar{f} \gamma_{\mu} \gamma^{5} f$$

EFT coupling with the SM fermion (nucleon)

For photon to axion/ALP conversion (reverse), see e.g.:

N. Song, L. Su, and L. Wu, 2402.15144; R. Perna, W. C. G. Ho, L. Verde, M. van Adelsberg,and R. Jimenez, 1201.5390

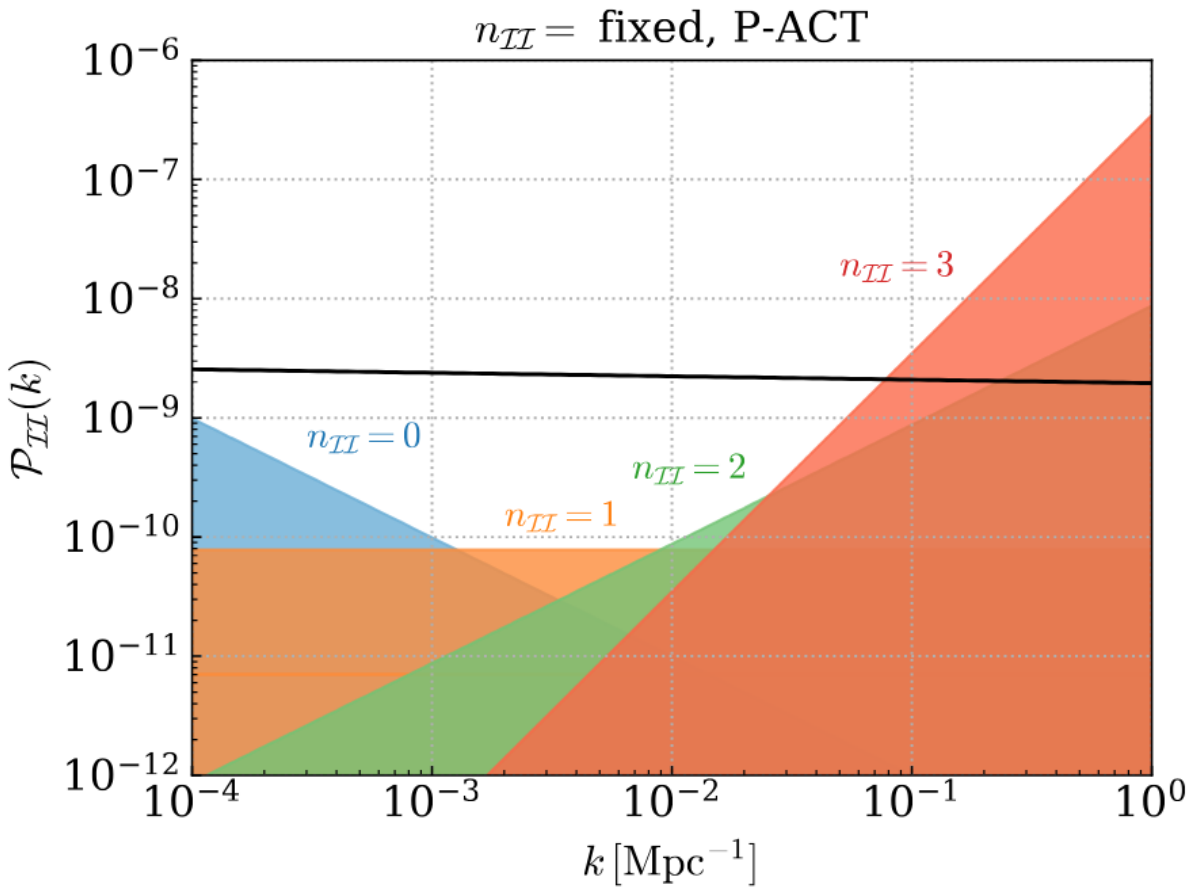
Inflationary Era and Axion DM

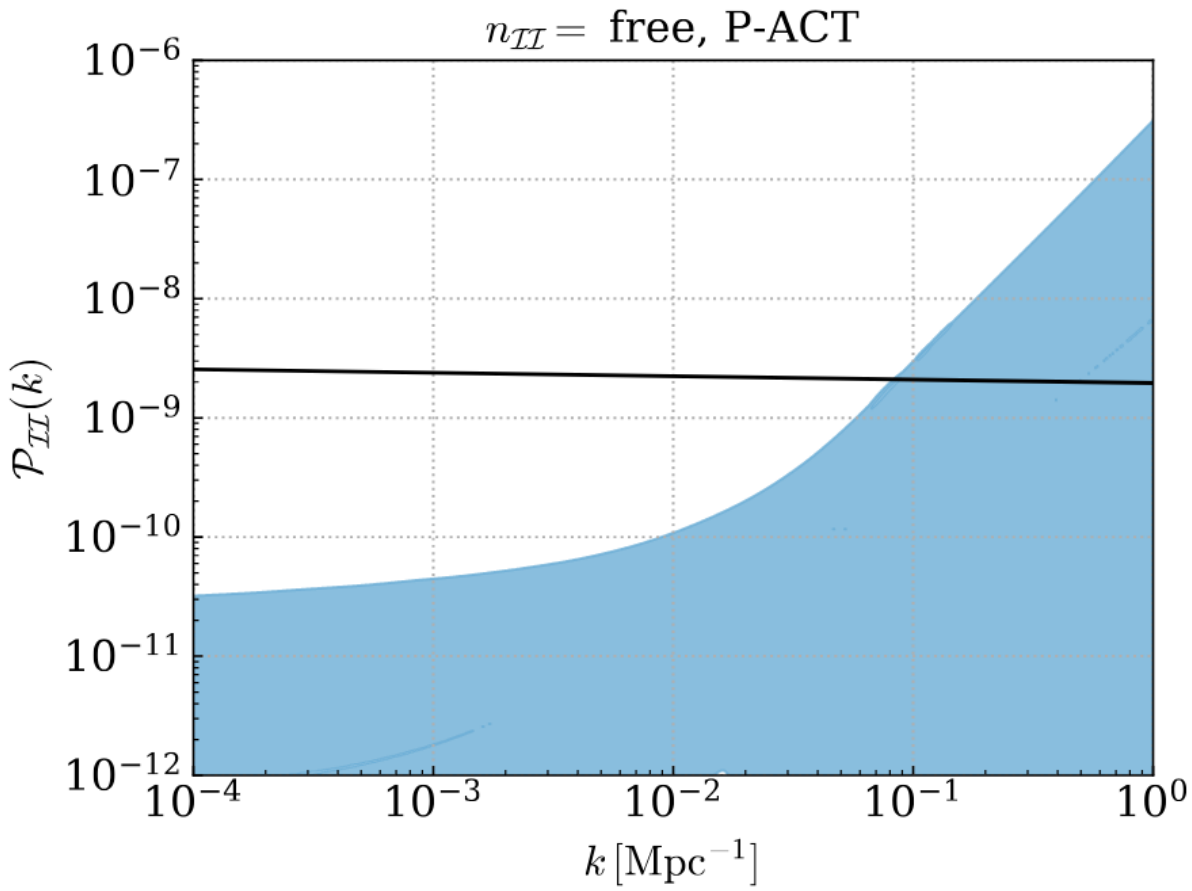


X. Chen, M. Braglia J. Fan, LFL, C. Preteti, P. Singh, In prep; X. Chen, J. Fan, LFL, 2303.03406; Y. Bao, J. Fan, LFL, 2209.09908;

But that will be another (long) story…

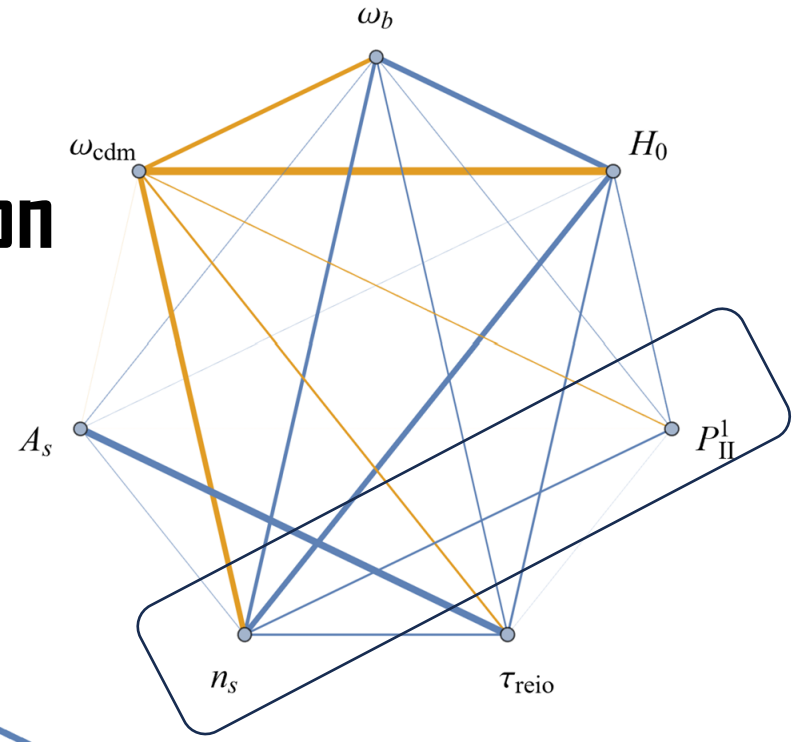
Recent Along the Line: (Axionic Blue Isocurvature)



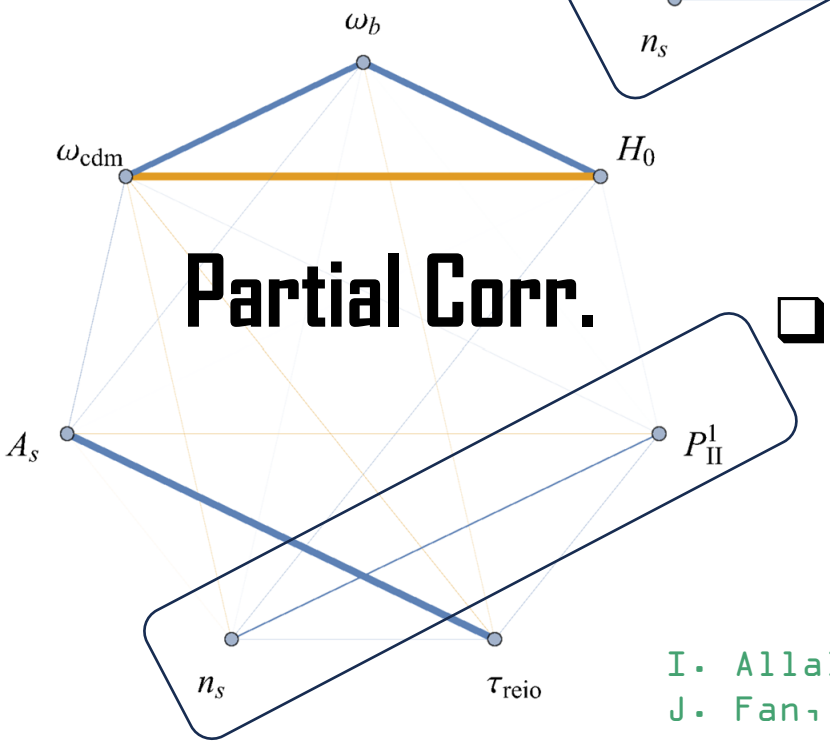


M. Braglia, X. Chen, J. Fan, LFL, C. Petretti, P. Singh, 2606.11312

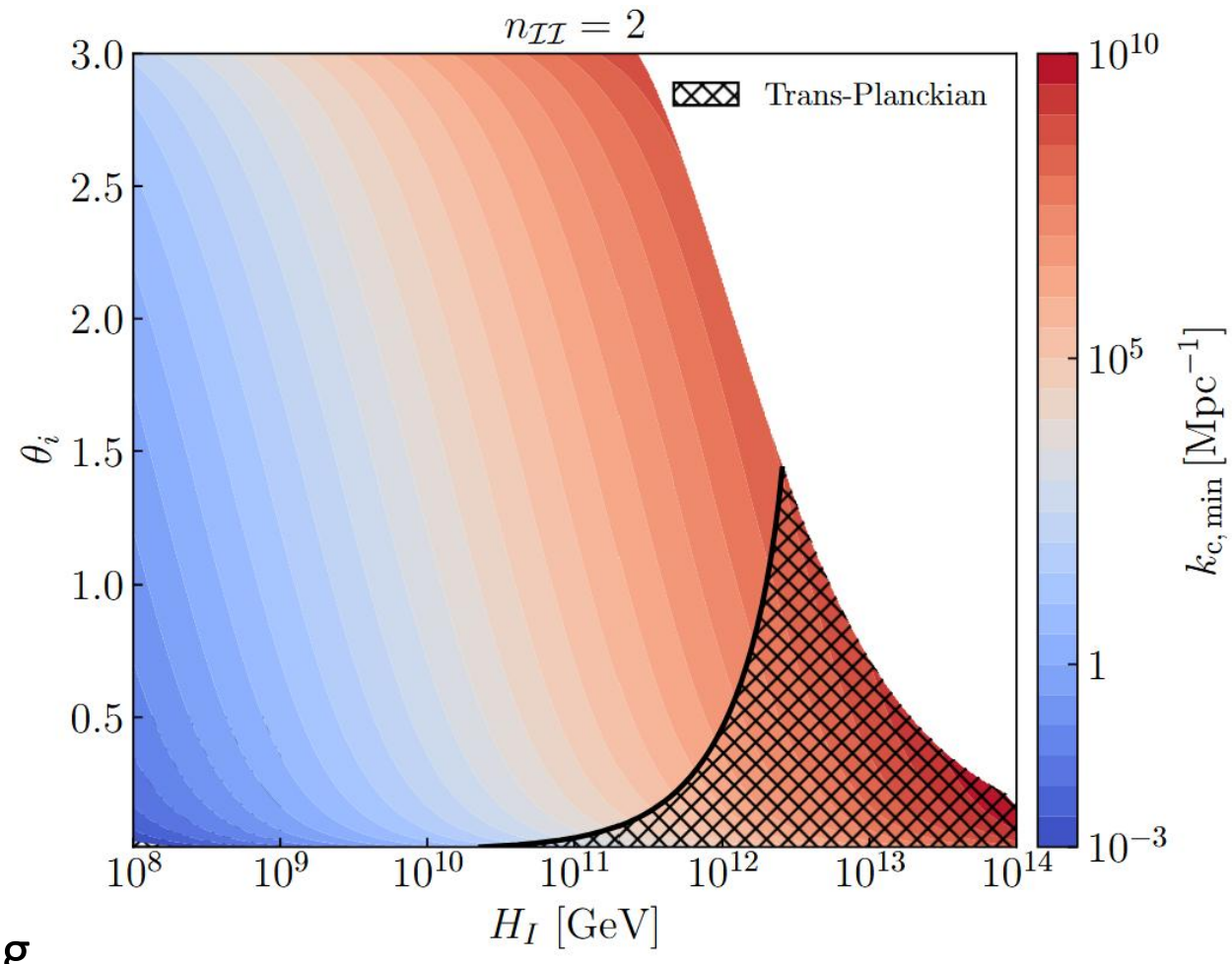
Pearson Correlation



Partial Corr.



- Preference on higher n_s softening isocurvature limits



- Scales of dynamic features and trans-Planckian initial conditions

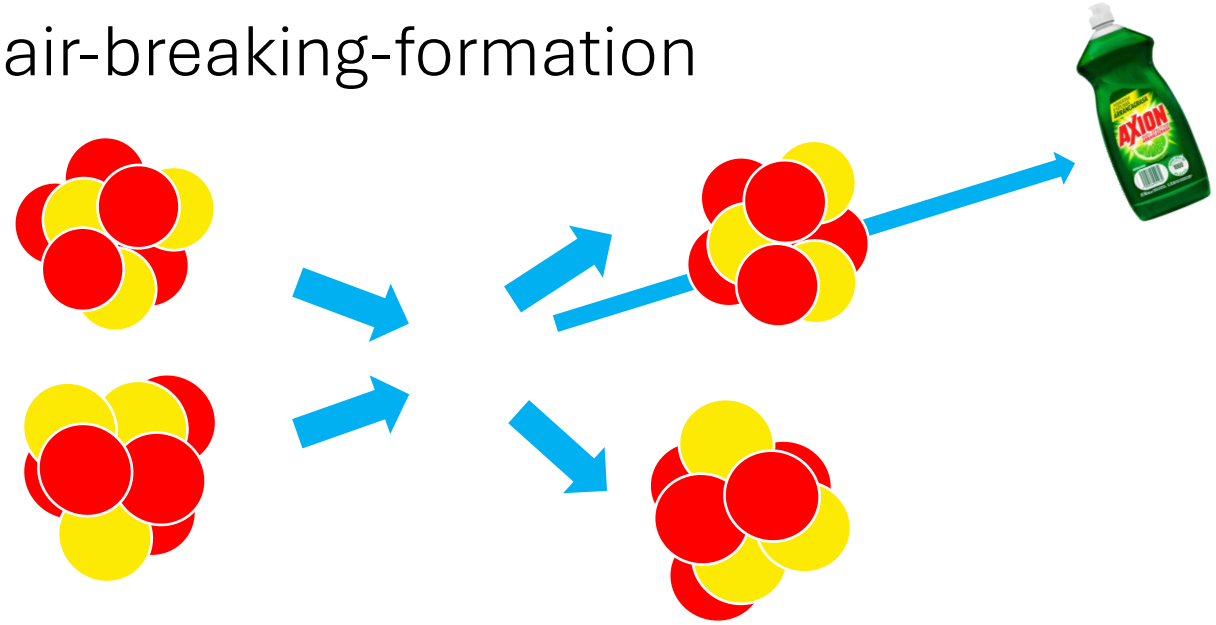
I. Allali, LFL, P. Singh, J. Fan, 2509.09678

Neutron Star(NS) as an ALP Source

The hot, dense core (T ~ keV) of NS could generate ALP through multiple mechanisms

- ❑ Nucleon scattering/emission processes
- ❑ Cooper pair-breaking-formation
- ❑ .....

$> 10^{30}$ ALP/s (?)



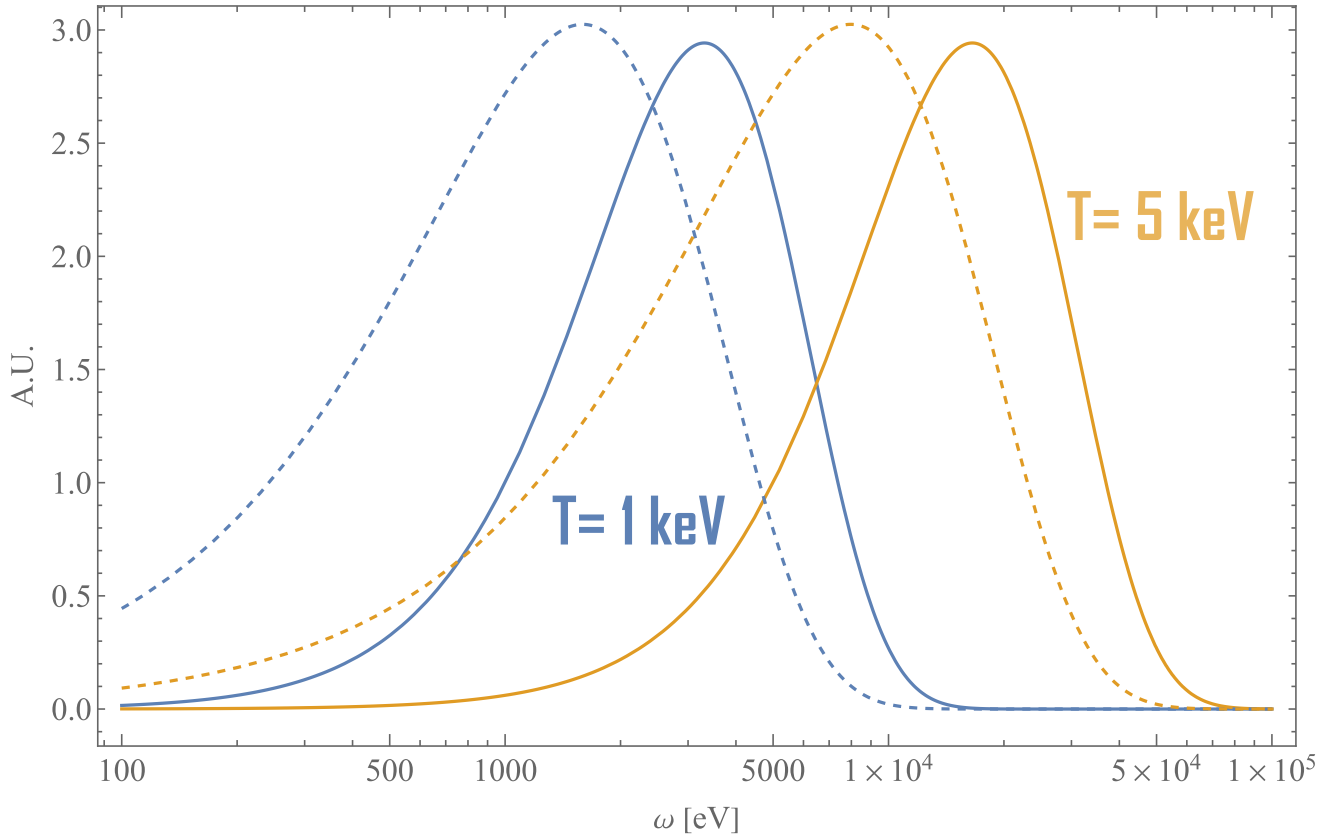
G. Raffelt, 1996; D. Yakovlev, K. Levenfish and Y. Shibanov, 1999; J. Keller and A. Sedrakian, 2012; A. Sedrakian, 2015; B.J. F. Fortin, H. K. Guo, S.P. Harris, D. Kim, K. Sinha and C. Sun, 2021;

Production Rate

The axion production rate & spectrum

$$\frac{dL_{nn}^{\infty}}{d\omega_a^{\infty}} = \frac{1}{9\pi^6} C_\pi \left(\frac{m_N}{m_\pi}\right)^4 f^4 g_{aN}^2 \frac{\omega_a^{\infty,3}(\omega_a^{\infty,2} + 4\pi^2 T^{\infty,2})}{e^{\omega_a^{\infty}/T^{\infty}} - 1}$$

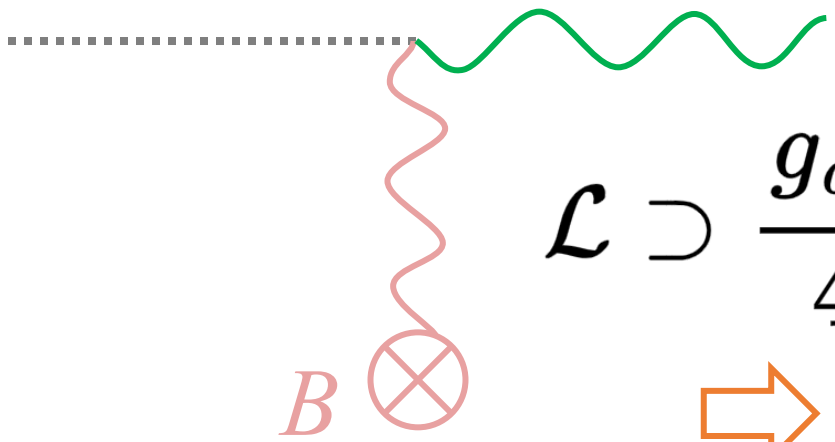
$$\times \int_0^{R_{\rm crust}} dr \frac{r^2}{\sqrt{1 - \frac{2Gm(r)}{r}}} p_{Fn}(r) F[c(r)] e^{-4\phi(r)}$$



Significantly harder than a thermal (black body) component of the same temperature

ALP Conversion in Strong Magnetic Fields

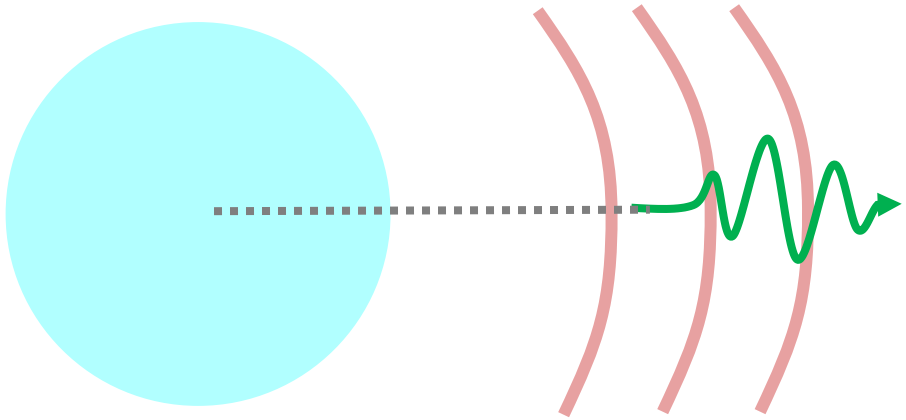
G. Raffelt and L. Stodolsky, 1988
D. Lai and J. Heyl, 2006;



$$\mathcal{L} \supset \frac{g_{a\gamma}}{4} a F^{\mu\nu} \tilde{F}_{\mu\nu}$$

$$\Rightarrow \propto a\, \mathbf{E} \cdot \mathbf{B}$$

- The strong magnetic field makes axion being converted to the Ordinary mode (O-mode) photon



- The mixing matrix between axion, the O- and X-modes:

$$i\frac{d}{dx}\begin{pmatrix} a \\ E_\parallel \\ E_\perp \end{pmatrix} = \begin{pmatrix} \omega R + \Delta_a R & \Delta_M R & 0 \\ \Delta_M R & \omega R + \Delta_\parallel R & 0 \\ 0 & 0 & \omega R + \Delta_\perp R \end{pmatrix} \begin{pmatrix} a \\ E_\parallel \\ E_\perp \end{pmatrix}$$

Axion Conversion in Strong Magnetic Fields

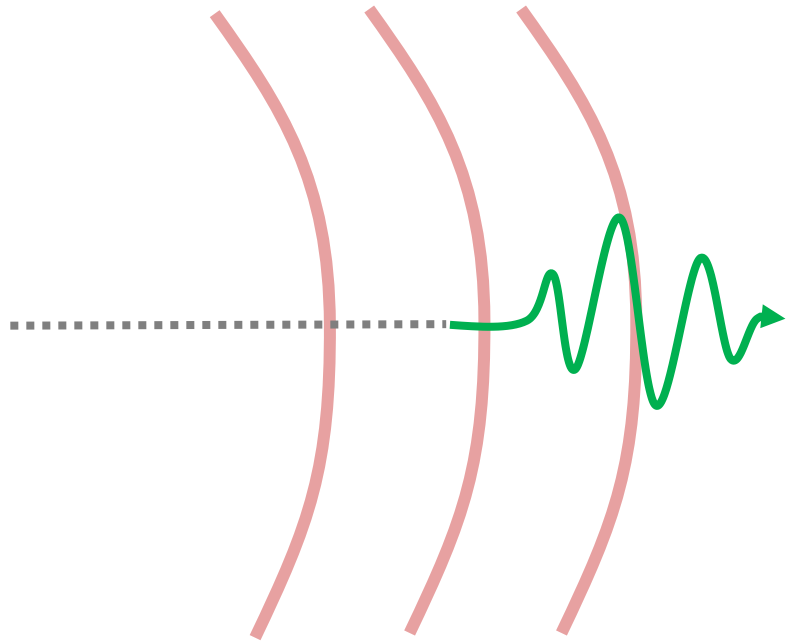
D. Lai and J. Heyl, 2006;
G. Raffelt and L. Stodolsky, 1988

$$i\frac{d}{dx}\begin{pmatrix} a \\ E_\parallel \\ E_\perp \end{pmatrix} = \begin{pmatrix} \omega R + \Delta_a R & \Delta_M R & 0 \\ \Delta_M R & \omega R + \Delta_\parallel R & 0 \\ 0 & 0 & \omega R + \Delta_\perp R \end{pmatrix} \begin{pmatrix} a \\ E_\parallel \\ E_\perp \end{pmatrix}$$

$\Delta_a = -\frac{m_a^2}{2\omega}$: ALP mass term, negligible for now

$\Delta_\parallel \simeq \frac{7\alpha}{45\pi}\frac{B^2\omega\sin^2\theta}{B_c^2}$: from vacuum polarization, dominates near the NS

$\Delta_M = \frac{g_{a\gamma}B\sin\theta}{2}$: Mixing term, changes slowly



Axion Conversion in Strong Magnetic Fields

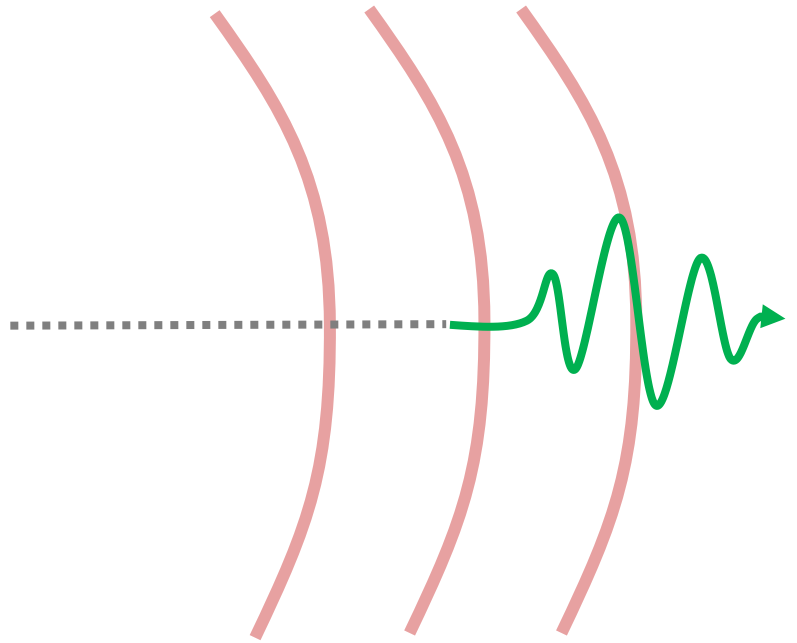
D. Lai and J. Heyl, 2006;
G. Raffelt and L. Stodolsky, 1988

$$i\frac{d}{dx}\begin{pmatrix} a \\ E_\parallel \\ E_\perp \end{pmatrix} = \begin{pmatrix} \omega R + \Delta_a R & \Delta_M R & 0 \\ \Delta_M R & \omega R + \Delta_\parallel R & 0 \\ 0 & 0 & \omega R + \Delta_\perp R \end{pmatrix} \begin{pmatrix} a \\ E_\parallel \\ E_\perp \end{pmatrix}$$

$\Delta_a = -\frac{m_a^2}{2\omega}$: ALP mass term, negligible for now

$\Delta_\parallel \simeq \frac{7\alpha}{45\pi}\frac{B^2\omega\sin^2\theta}{B_c^2}$: from vacuum polarization, dominates near the NS

$\Delta_M = \frac{g_{a\gamma}B\sin\theta}{2}$: Mixing term, changes slowly



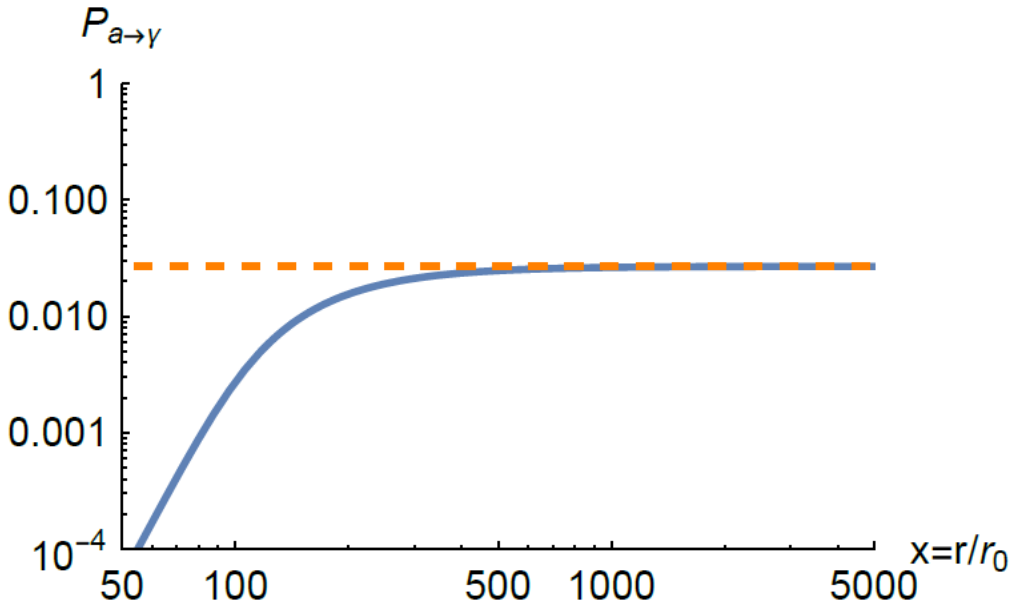
$$
\begin{aligned}
P_{a\to\gamma}(x) &\approx \left|\int_1^x dx' \Delta_M(x') r_0 \exp\left(i\Delta_a r_0 \left(x' - \frac{x_c}{5}\left(\frac{x_c}{x'}\right)^5\right)\right)\right|^2 \\
&= \frac{(\Delta_M(1) r_0)^2}{x_c^4}\left|\int_{1/x_c}^{x/x_c} \frac{dt}{t^3} \exp\left(i\Delta_a r_0 x_c \left(t - \frac{1}{5t^5}\right)\right)\right|^2 \\
&\approx \frac{(\Delta_M(1) r_0)^2}{x_c^4}\left|\int_{1/x_c}^{x/x_c} \frac{dt}{t^3} \exp\left(i\Delta_a r_0 x_c \left(-\frac{1}{5t^5}\right)\right)\right|^2 \\
&= \frac{(\Delta_M(1) r_0)^2}{5^{\frac{6}{5}} |\Delta_a r_0 x_c|^{\frac{4}{5}} x_c^4} \times \\
&\quad \left|\Gamma\left(\frac{2}{5}, \frac{i\Delta_a r_0 x_c}{5(x/x_c)^5}\right) - \Gamma\left(\frac{2}{5}, \frac{i\Delta_a r_0 x_c}{5(1/x_c)^5}\right)\right|^2
\end{aligned}
$$

ALP Conversion in Strong Magnetic Fields (II)

Near the NS, where the B field is extreme,

Mixing **only** happens far from the surface

$$\frac{r_{\rm con}}{r_0} = 85 \left(\frac{\omega}{3\,{\rm keV}}\right)^{\frac{1}{5}} \left(\frac{B_0}{10^{13}\,{\rm G}}\right)^{\frac{2}{5}} \left(\frac{r_0}{12\,{\rm km}}\right)^{\frac{1}{5}} (\sin\theta)^{\frac{2}{5}}$$



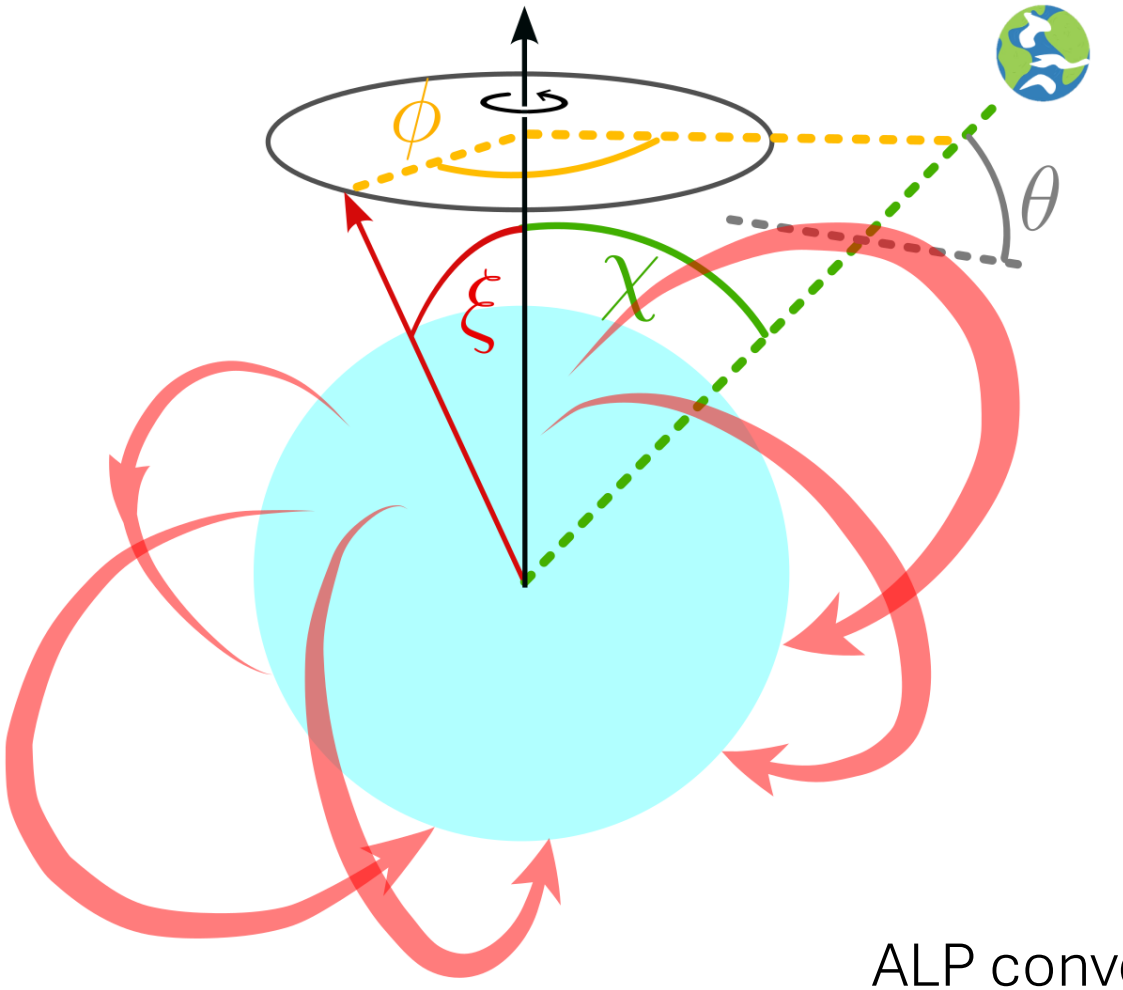
$$p_{a\to\gamma} \approx 1.5\times 10^{-4} \left(\frac{g_{a\gamma\gamma}}{10^{-11}\ {\rm GeV}^{-1}}\right)^2 \left(\frac{1\ {\rm keV}}{\omega}\right)^{4/5} \left(\frac{B_0}{10^{13}\ {\rm G}}\right)^{2/5} \left(\frac{R_{\rm NS}}{10\ {\rm km}}\right)^{6/5} \sin^{2/5}\theta\,,$$

Robust against non-dipole and GR corrections

See also:

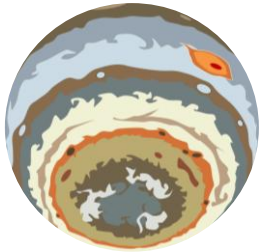
C. Dessert, D. Dunsky and B.R. Safdi, 2022; E. Gau, F. Hajkarim, S. P. Harris, P. S. B. Dev, J. F. Fortin, H. Krawczynski and K. Sinha, 2023

Geometry of the System



- Our line of sight (LOS) doesn't align with the NS's spin axis, leaving a non-zero χ
- The magnetic dipole is also not guaranteed to align with the spin axis, giving another angle ξ
- The phase ϕ



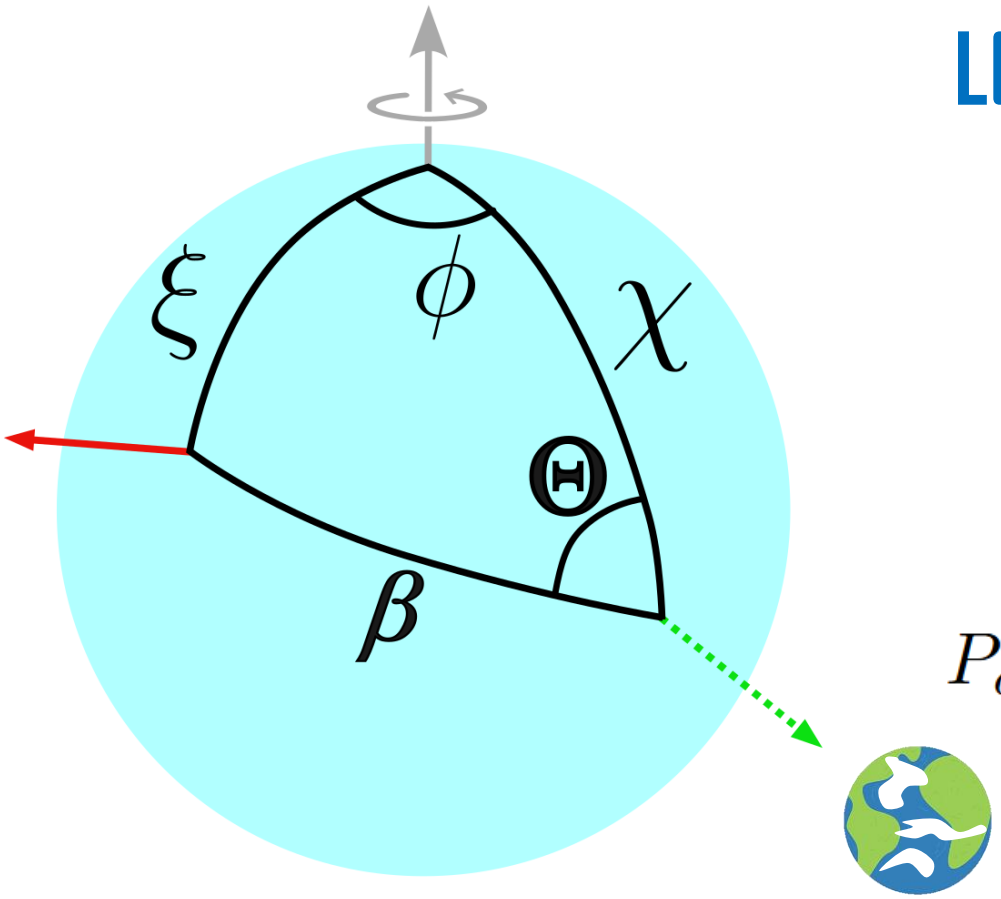


$$\xi \simeq 0.2$$

J. Fan, LFL, JHEP 10, 186 (2022); S. Yan , LFL , J. Fan, JHEP 06, 028 (2024); P. Singh, S. Yan, I. Allali, LFL, J. Fan, JCAP 09, 019, (2024)

ALP conversion always gives the O mode, but the O mode needs to be defined "locally"

Spherical Trigonometry



The conversion only depend on the LOS angle relative to the dipole (β)

$$\cos\beta = \cos\xi\cos\chi + \sin\xi\sin\chi\cos\phi$$

$$\tan\Theta = \frac{\sin\phi\sin\xi}{\cos\chi\sin\xi\cos\phi - \sin\chi\cos\xi}$$

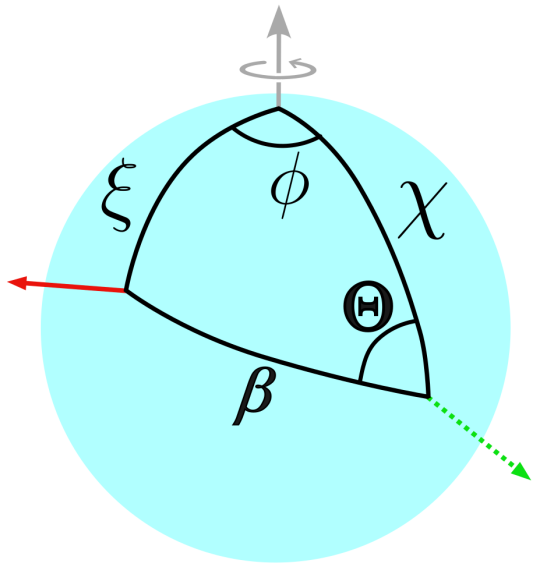
Mudulated intensity: the pulse

$$P_{a\to\gamma} \propto (B_0\sin\theta)^{2/5}$$

$$\propto \sin\beta^{2/5}$$

$$= [1-(\cos\xi\cos\chi + \sin\xi\sin\chi\cos\phi)^2]^{1/5}$$

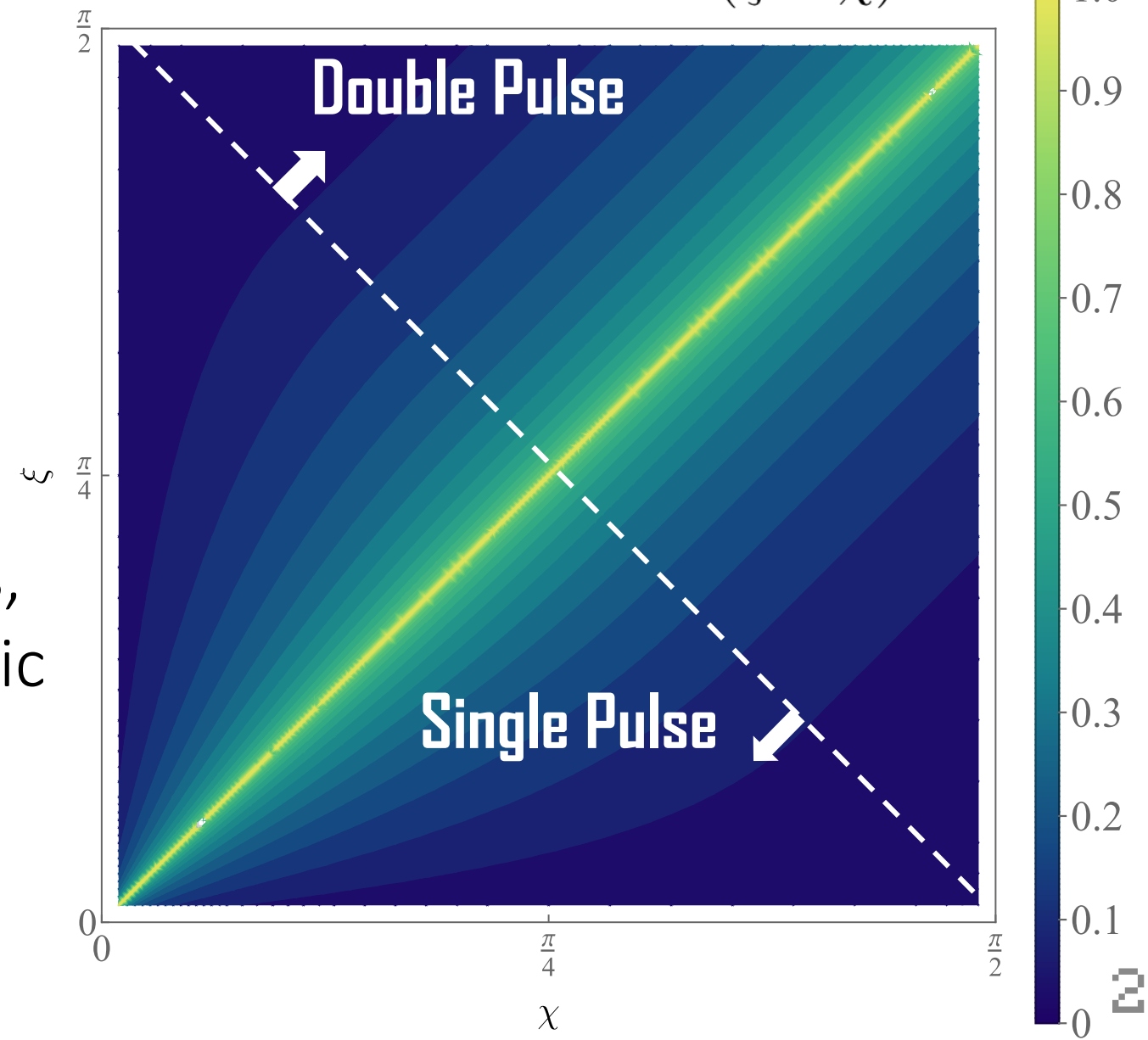
Pulse Fraction



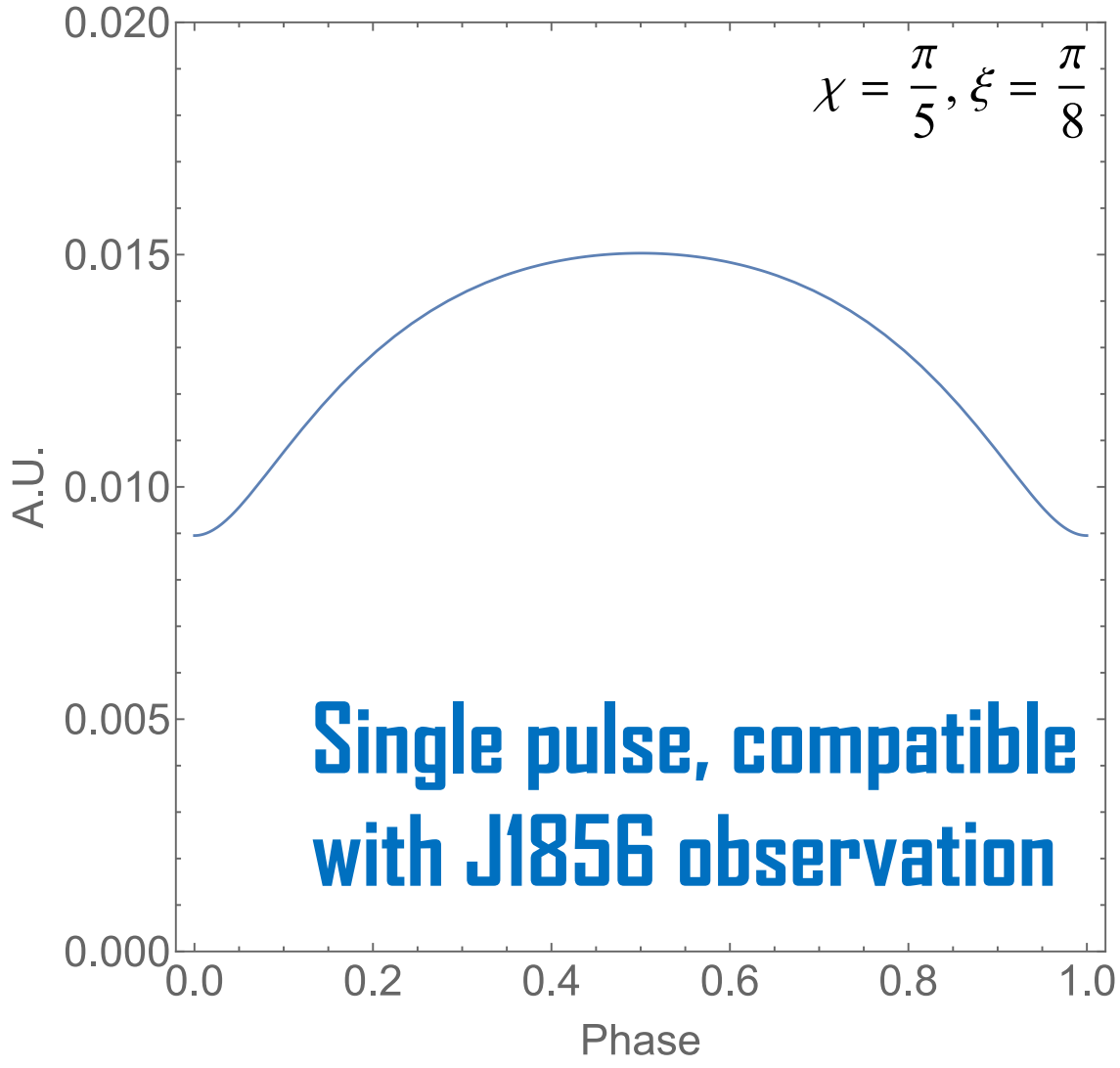
- Without polarization probes, the two angles are symmetric under exchange

$$\mathrm{PF} = \frac{\sin^{2/5}(\xi+\chi) - \sin^{2/5}(\xi-\chi)}{\sin^{2/5}(\xi+\chi) + \sin^{2/5}(\xi-\chi)}$$

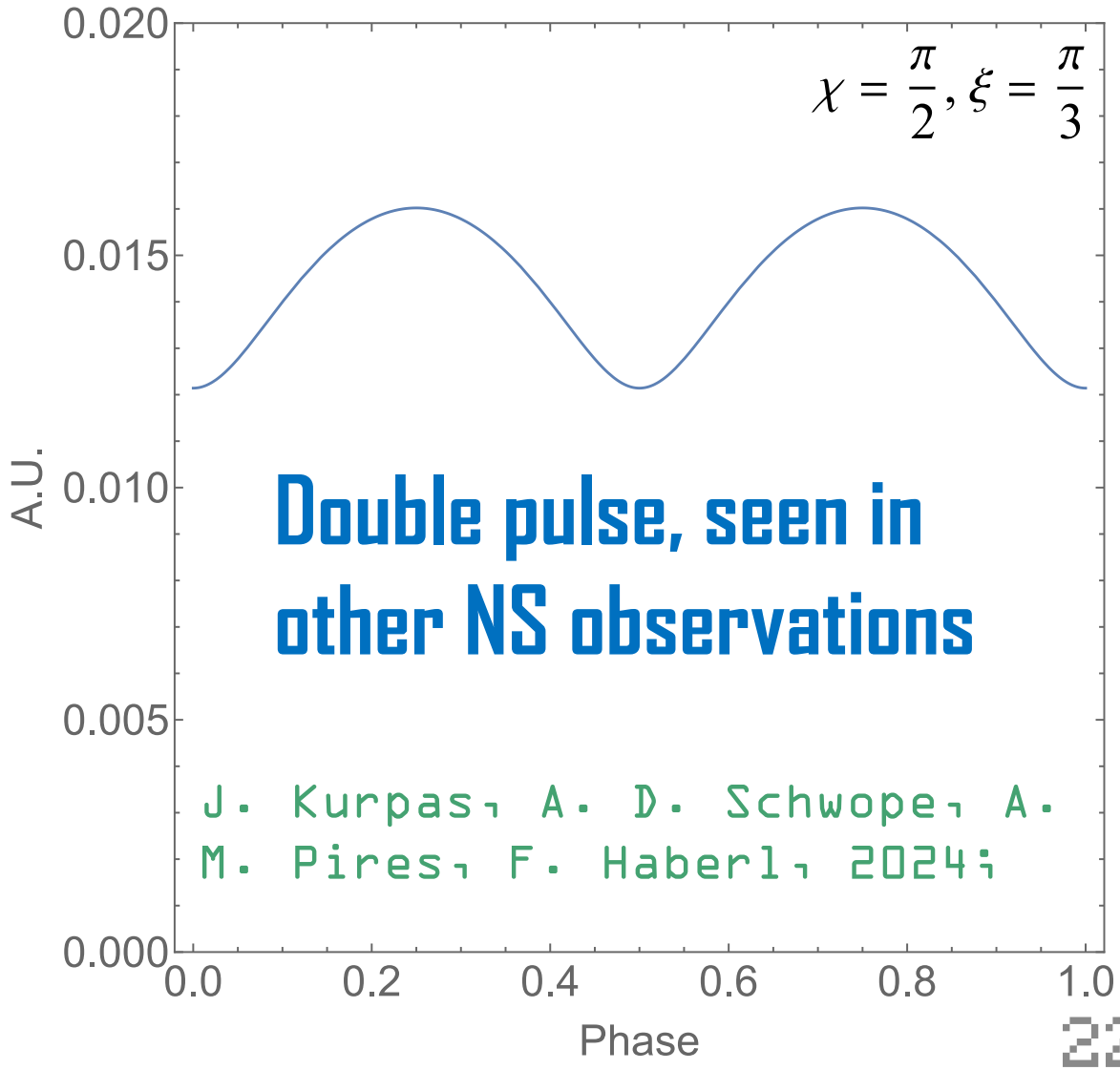
$$\mathrm{PF} = \frac{1 - \sin^{2/5}(\xi-\chi)}{1 + \sin^{2/5}(\xi-\chi)}$$



Theoretical Prediction



Single pulse, compatible with J1856 observation

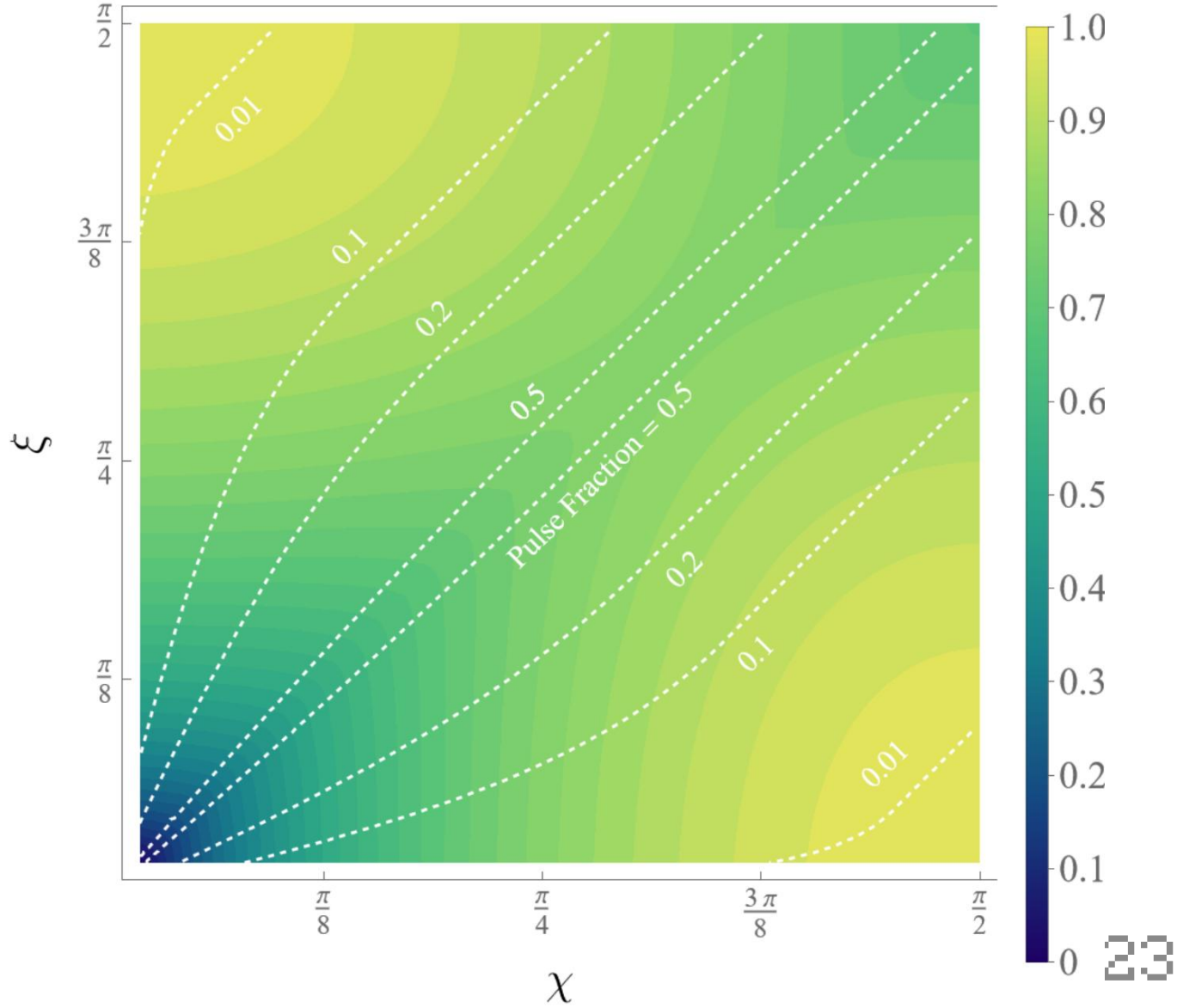


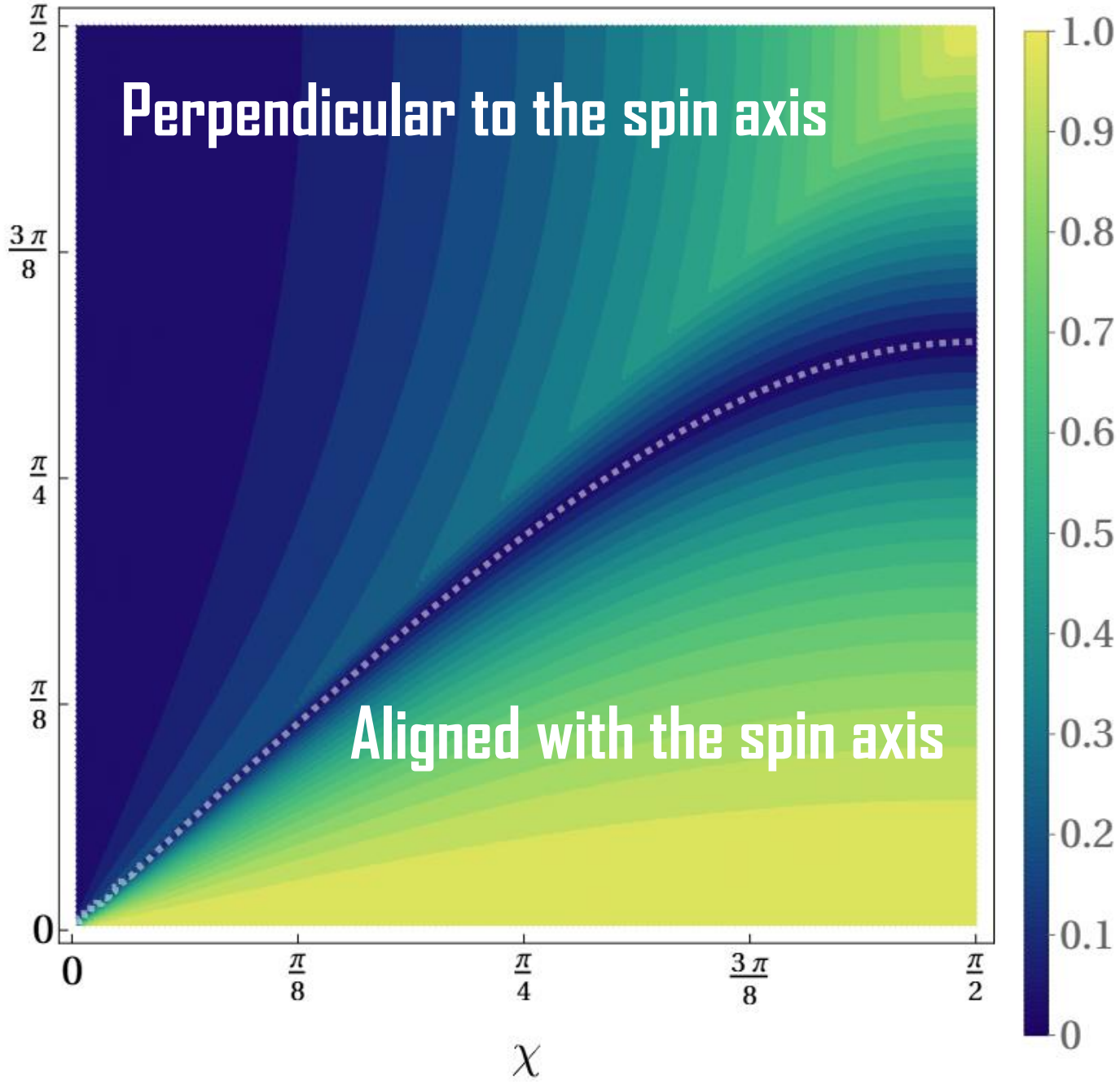
Double pulse, seen in other NS observations

J. Kurpas, A. D. Schwope, A. M. Pires, F. Haberl, 2024;

Average Attenuation Factor

The average flux obtained is weaker than the naïve estimation (O(1) correction)





Phase-integrated Polarization

$$\mathrm{PD} = \frac{\sqrt{Q^2+U^2}}{I}$$

$$= \left[\left\langle |\mathbf{A}|^2 \cos(2\Theta)\right\rangle^2 + \left\langle |\mathbf{A}|^2 \sin(2\Theta)\right\rangle^2\right]^{1/2} / \left\langle |\mathbf{A}|^2\right\rangle .$$

Uniformly applied to NS conversions of light ALPs

- ❑ Energy independent
- ❑ ALP mass independent
- ❑ Magnetic field independent

X-ray (Must) in Space









In the future

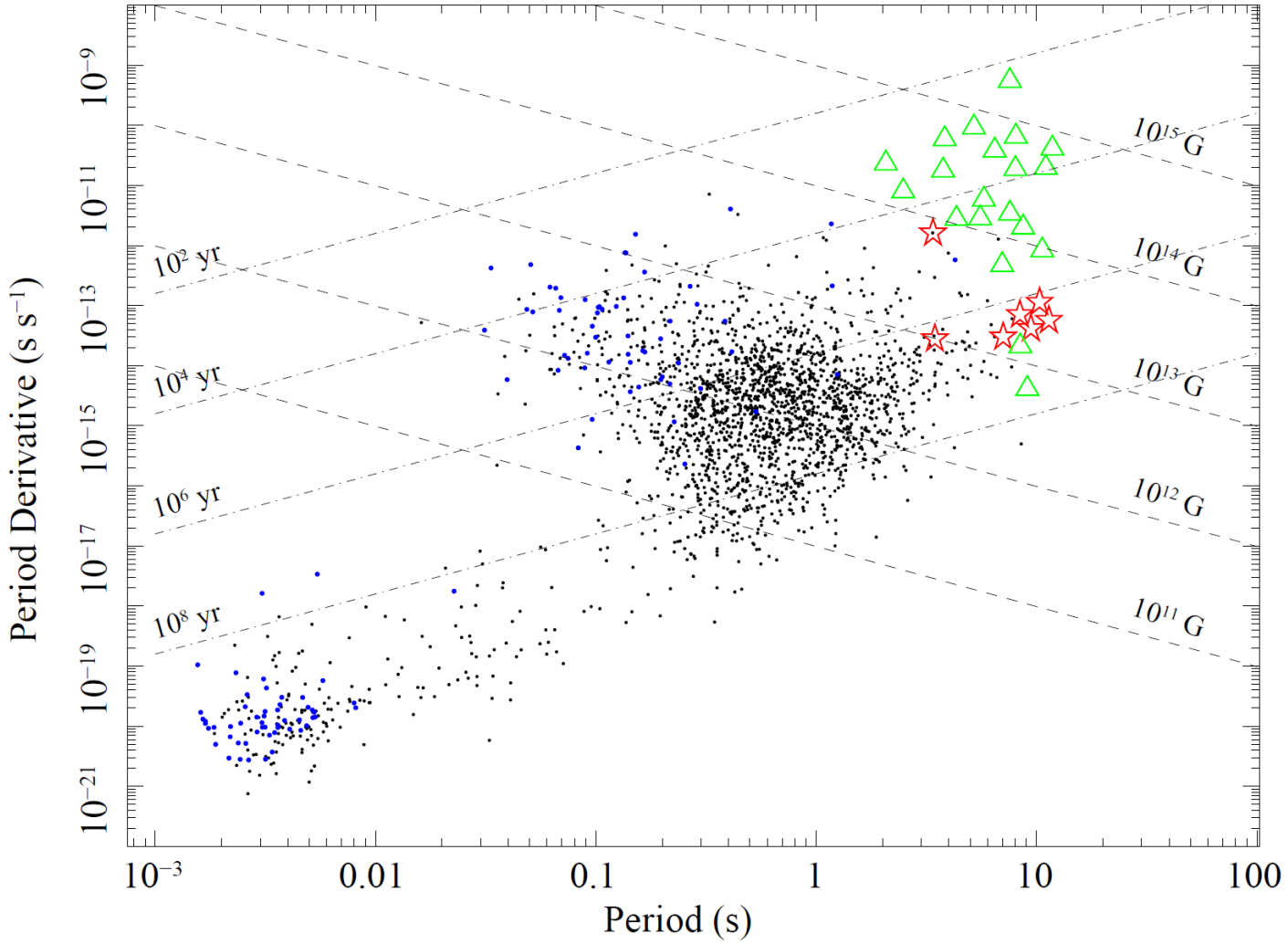


eXTP



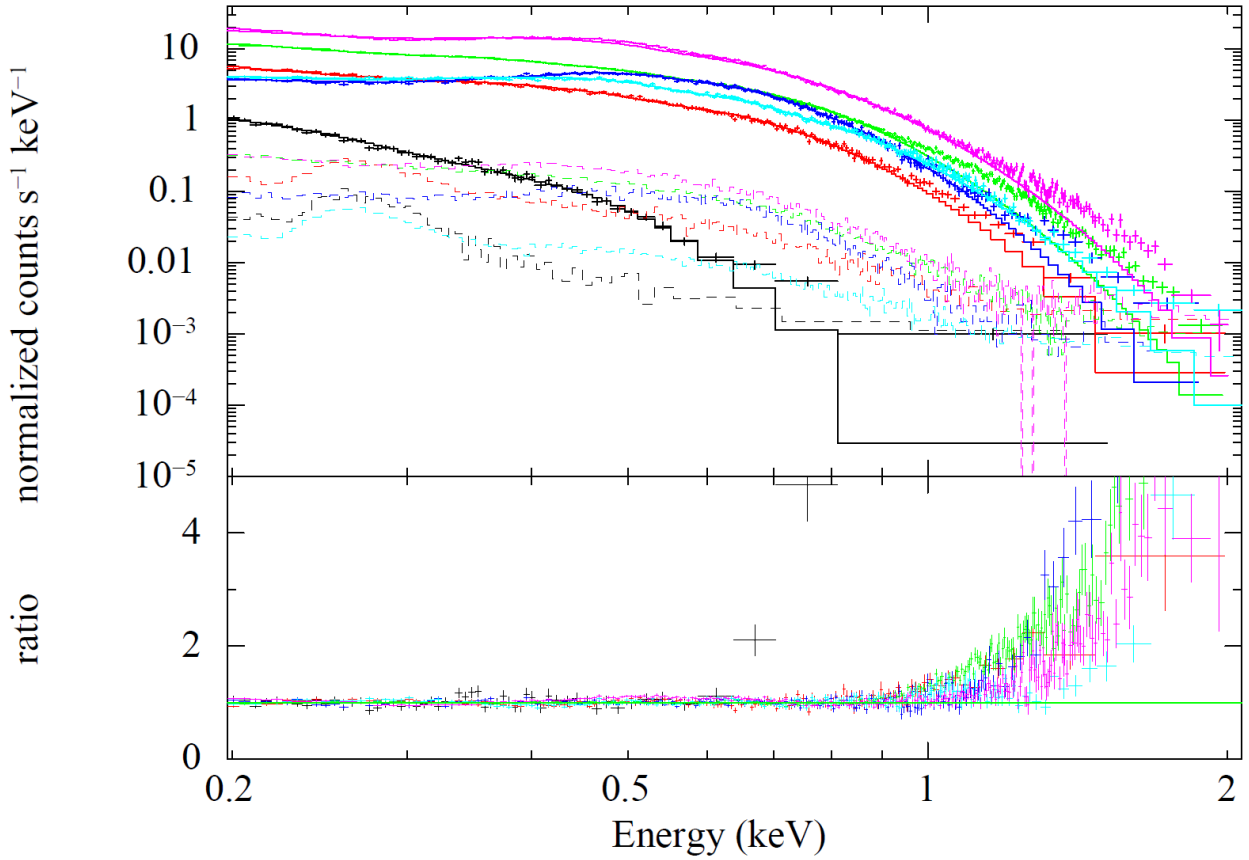
CATCH

Case Study: X-ray Dim Isolated NS (XDINS)



Case Study: X-ray Dim Isolated NS (XDINS)

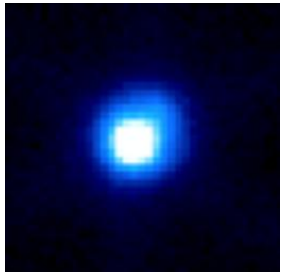
T. Yoneyama, K. Hayashida , H. Nakajima, H. Matsumoto, 1811.11982; C. Dessert, J. W. Foster, B. R. Safdi, 1910.02596



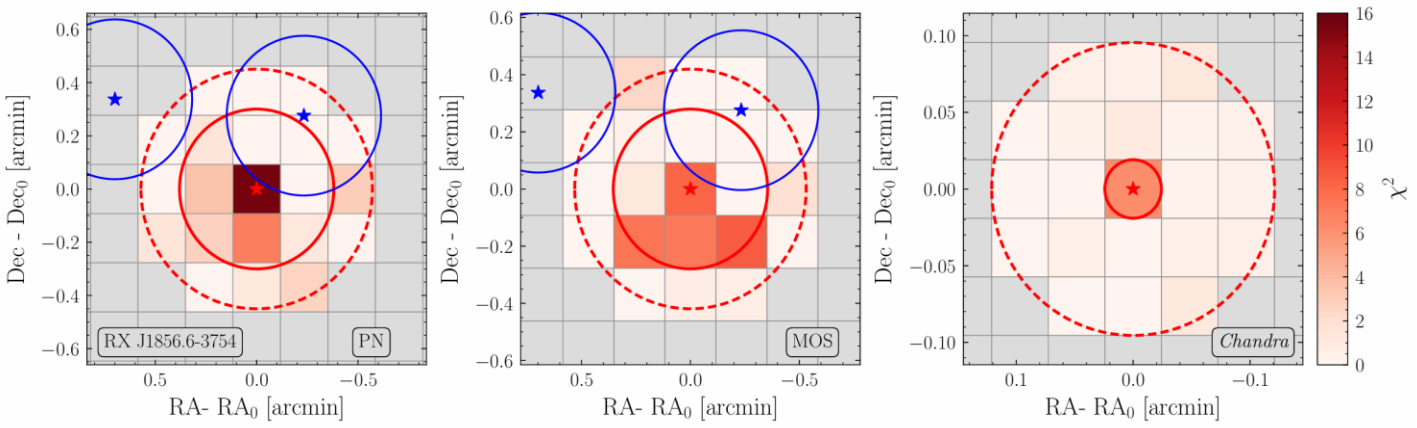
Also called “magnificent 7”

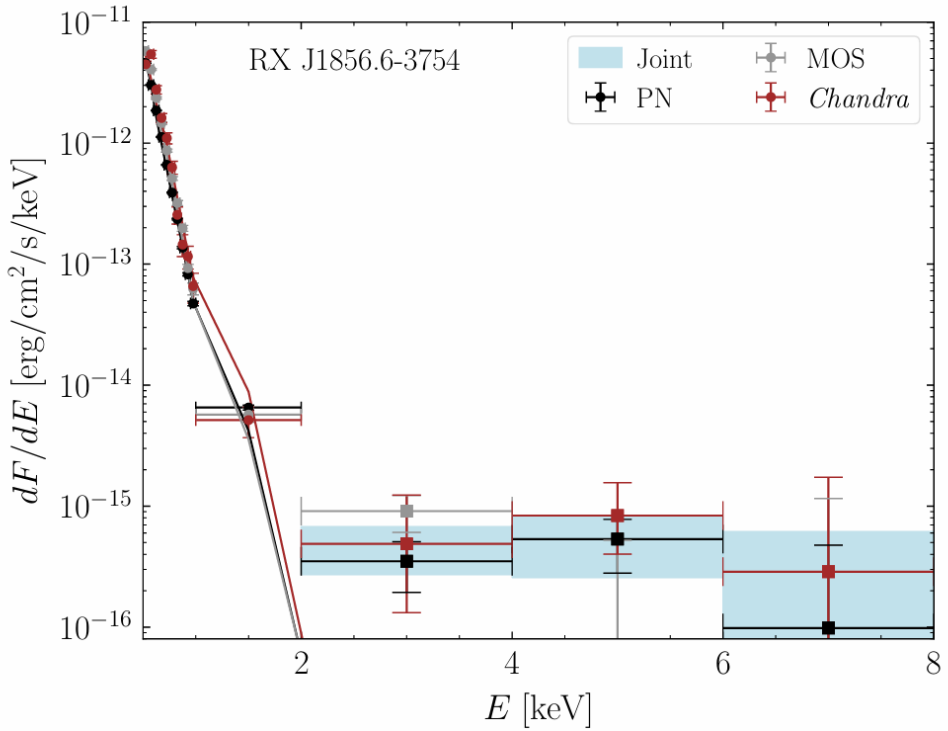
- B field: O(10^{13}) G
- Frequency: O(0.1) Hz
- Age: O (10^{5}) yrs
- Surface BB temperature: O(100) eV
- (Universal) non-thermal X-ray excess
- Rather dim sources

Hard X-ray Excess in RX J1856.6-3745



- Discovered in 1992
- One of the closest NS (~123 pc from us)



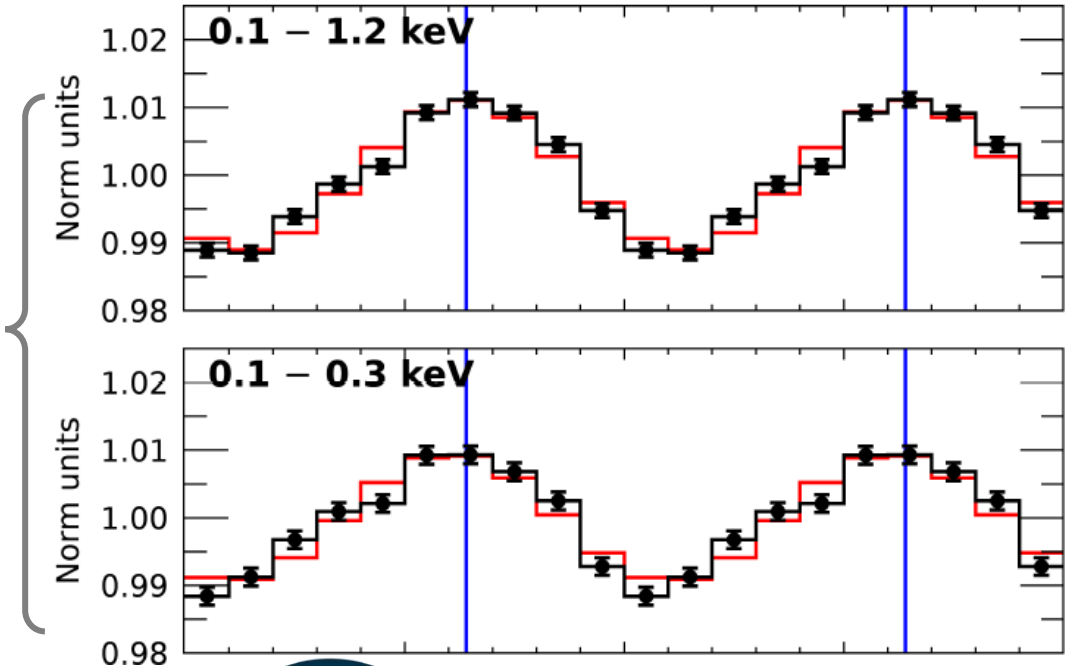


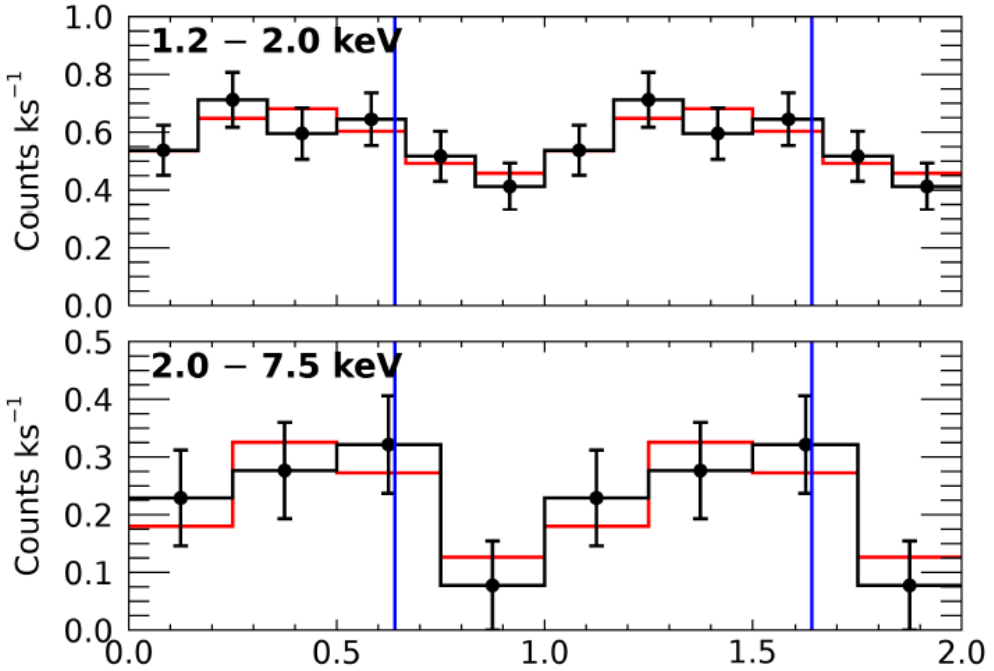
Observed in both XMM-Newton and Chandra, accumulated ~5σ excess

C. Dessert, J. W. Foster, B. R. Safdi, 1910.02596

Pulse Structure, from XDINS RX-J1856.5-3754

Pulse fraction goes up to ~50% at higher energies





1-2% pulse at low energies

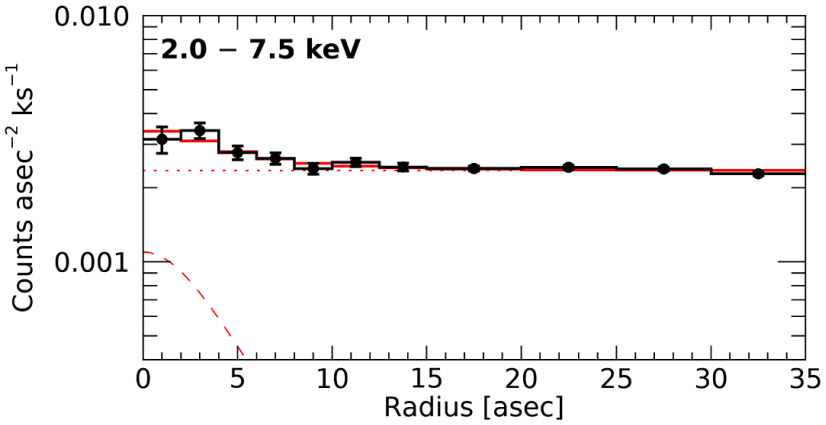




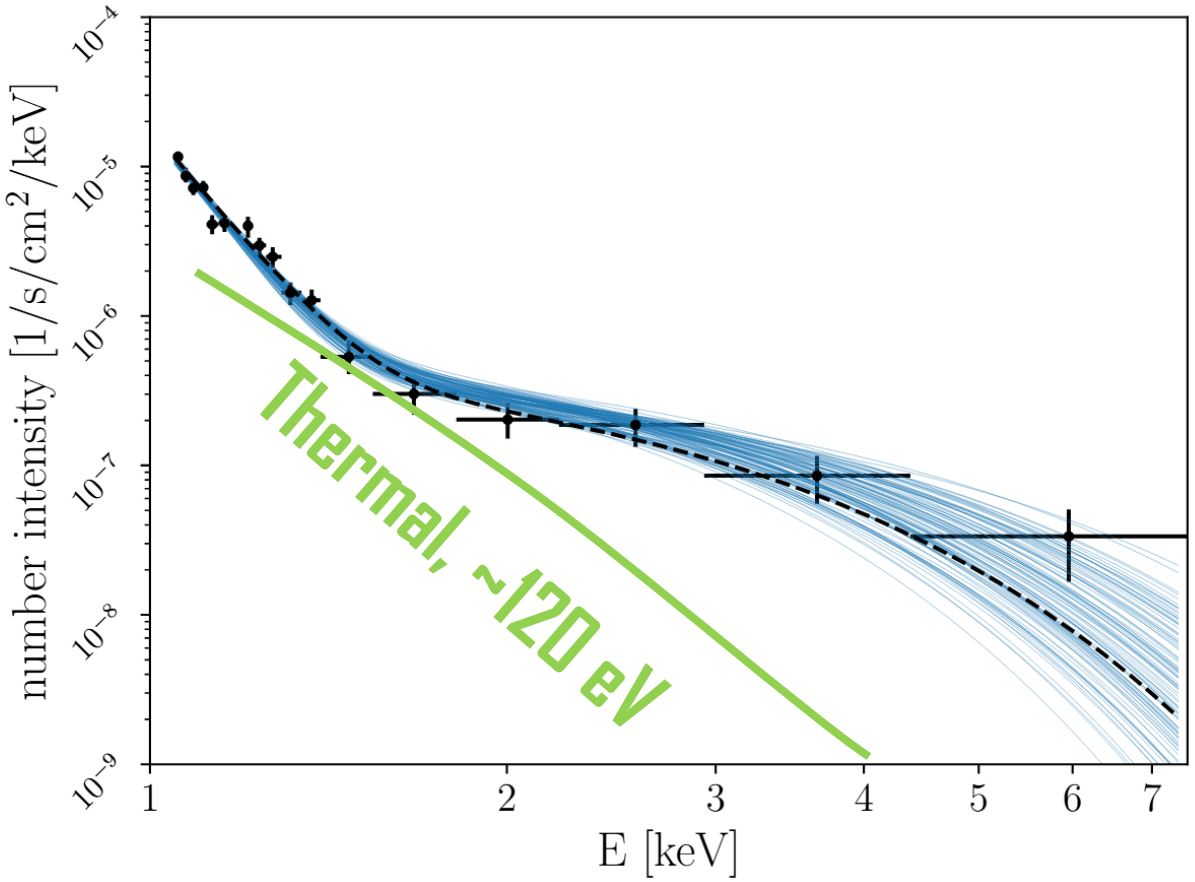
D. De Grandis, M. Rigoselli, S. Mereghetti, G. Younes, P. Pizzochero, R. Taverna, A. Tiengo, Rturolla, and S. Zane, 2022

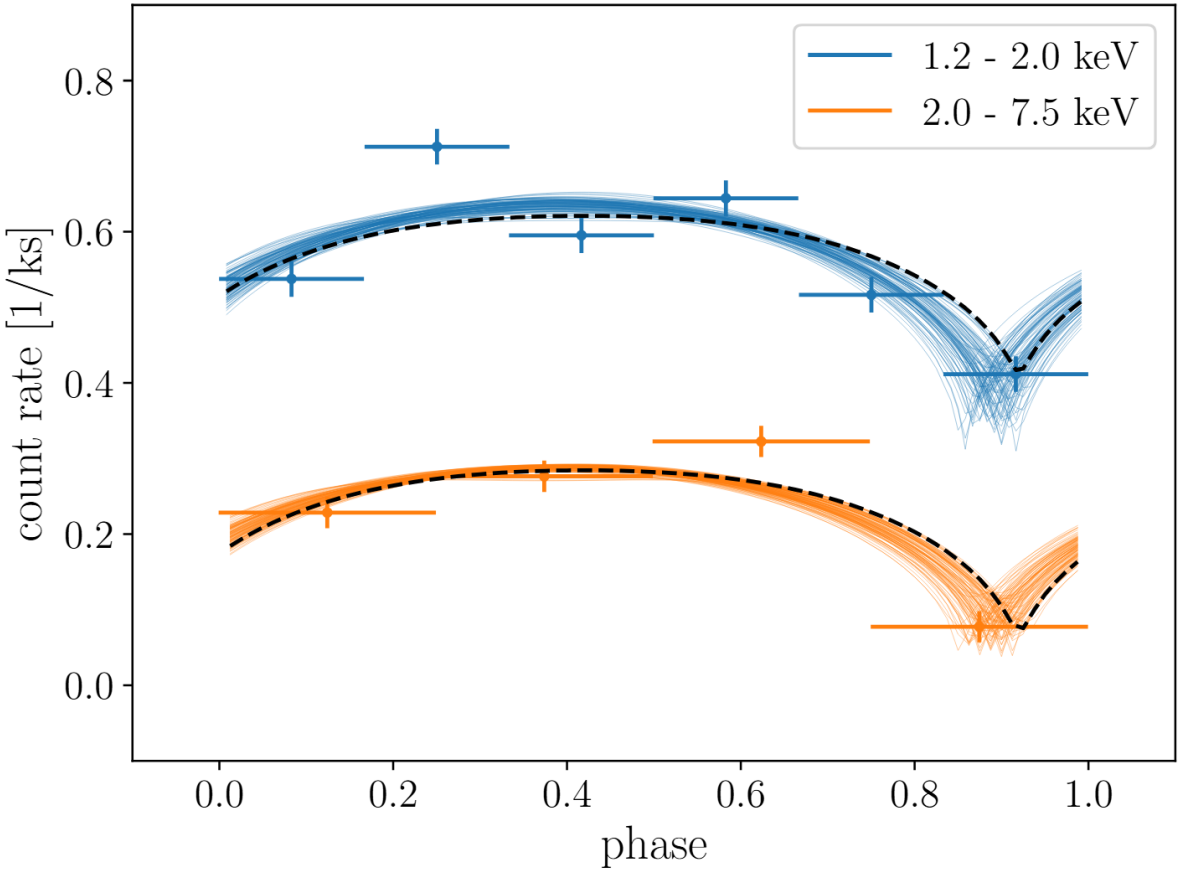
About the Data Used

- Major data from XMM-Newton Epic-pn camera, across 2 decades with 1.43 Ms
- Phase information (time stamps) are obtained from NICER
- Background subtracted (short-term flare noise and permeating backgrounds, giving rise to systematics at high energy.
- A soft black body (~62 eV) and a hard black body (~120 eV) is found, not able to explain the excess.



Limiting the Axion Param Space



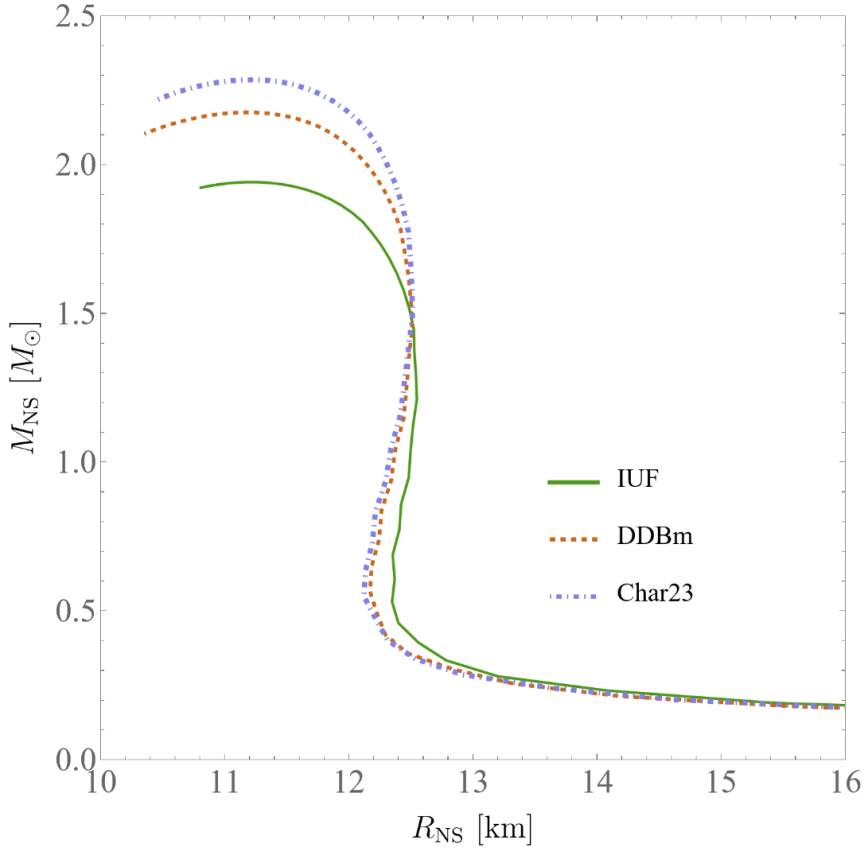


Phase error bars shrinked to mimic potential progress

Systematic Uncertainties

$$\frac{dL_{nn}^{\infty}}{d\omega_a^{\infty}} = \frac{1}{9\pi^6} C_\pi \left(\frac{m_N}{m_\pi}\right)^4 f^4 g_{aN}^2 \frac{\omega_a^{\infty,3}(\omega_a^{\infty,2} + 4\pi^2 T^{\infty,2})}{e^{\omega_a^{\infty}/T^{\infty}} - 1}$$
$$\times \int_0^{R_{\rm crust}} dr \frac{r^2}{\sqrt{1 - \frac{2Gm(r)}{r}}} p_{Fn}(r) F[c(r)] e^{-4\phi(r)}$$

Integrating Tolman-Oppenheimer-Volkoff equation with EOS, large uncertainties

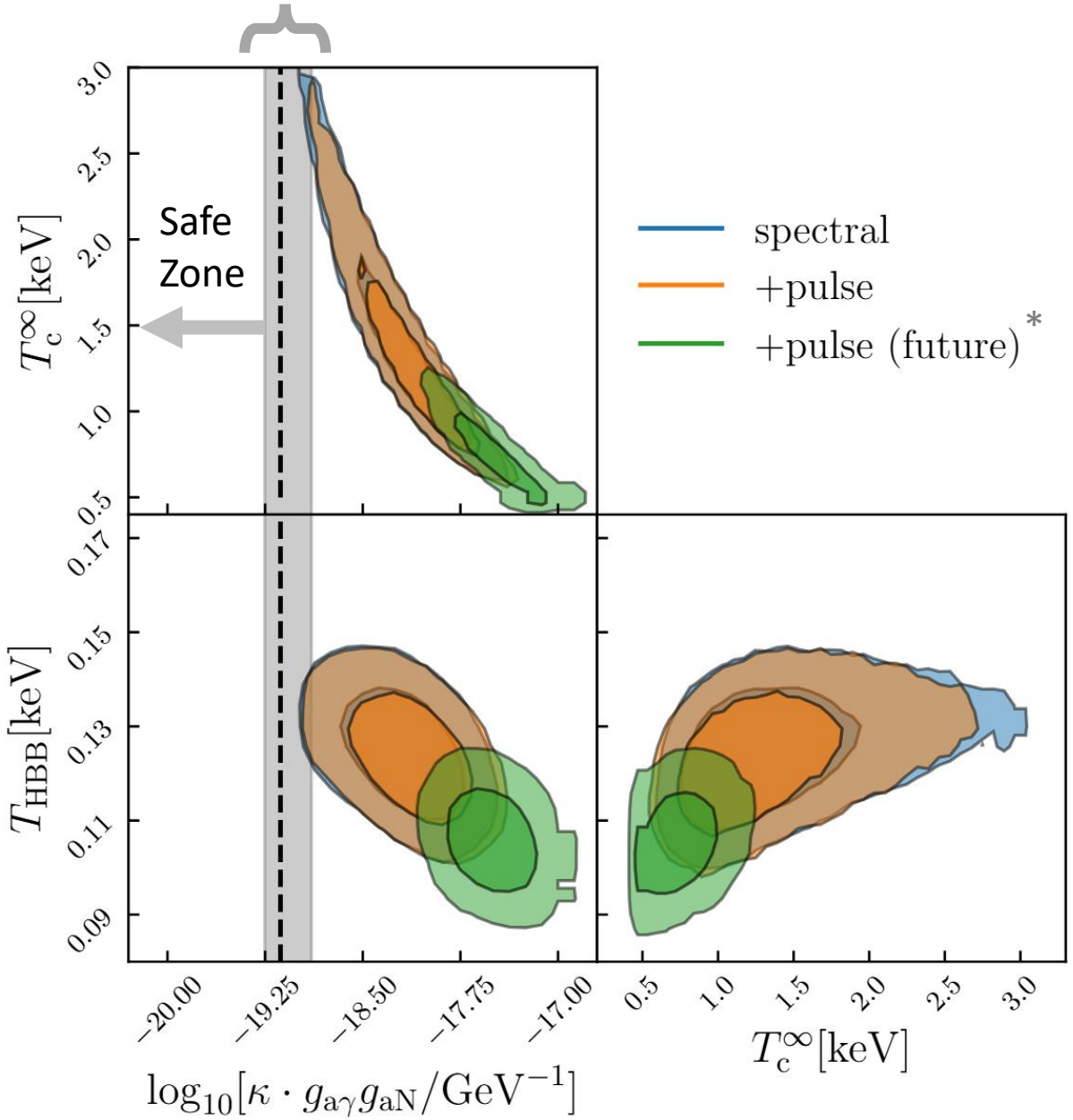


Other factors:

- ❑ B field: not very important as the 2/5 power suppression in conversion
- ❑ Distance: we got parallax
- ❑ Radius: not changing very much with mass

$M_{\rm NS}$ $[M_\odot]$	1.1	1.2	1.3	**1.4**	1.5	1.6	1.7	1.8	1.9
L_a $[L_{a,0}]$	1.70	2.05	2.48	**2.98**	3.58	4.32	5.29	6.62	8.91
$R_{\rm NS}$ [km]	12.8	12.8	12.8	12.7	12.7	12.6	12.4	12.2	11.8

Systematic Uncertainties!



Fit Result

Haven't projected the polarization measurement limits due to lacking prior knowledge

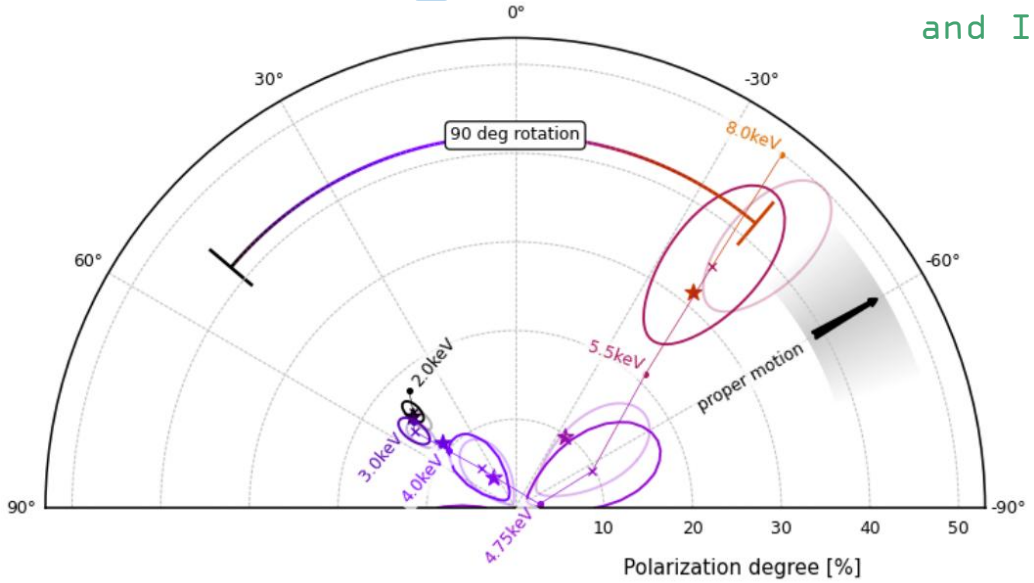
	$\mathrm{Log}(g \cdot g)$	T_c^∞ [keV]	$T_{\rm HBB}^\infty$ [keV]	ξ	χ
$\mathcal{Q}_1$	$-18.25^{+0.29}_{-0.33}$	$1.30^{+0.52}_{-0.32}$	$0.12^{+0.01}_{-0.01}$	$0.79^{+0.52}_{-0.53}$	$0.79^{+0.54}_{-0.53}$
$\mathcal{Q}_2$	$-18.19^{+0.28}_{-0.33}$	$1.26^{+0.50}_{-0.31}$	$0.12^{+0.01}_{-0.01}$	$0.72^{+0.46}_{-0.41}$	$0.73^{+0.46}_{-0.42}$
$\mathcal{Q}_3$	$-17.59^{+0.22}_{-0.22}$	$0.76^{+0.19}_{-0.15}$	$0.11^{+0.01}_{-0.01}$	$0.42^{+0.24}_{-0.20}$	$0.41^{+0.23}_{-0.20}$

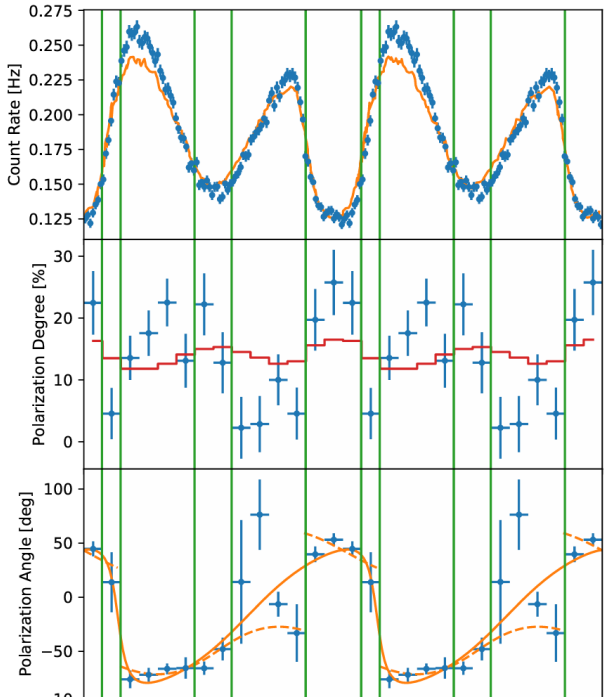
* Future pulse is obtained by shrinking the current error bars by a factor of 4

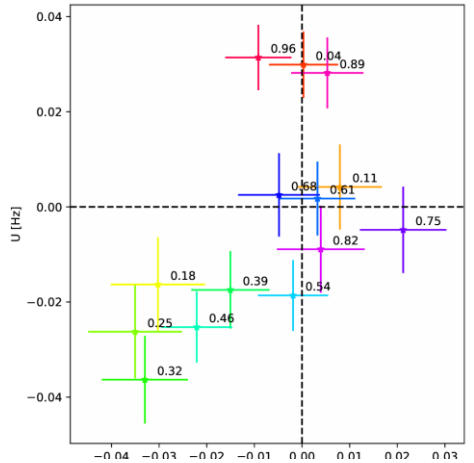
Another Interesting Target

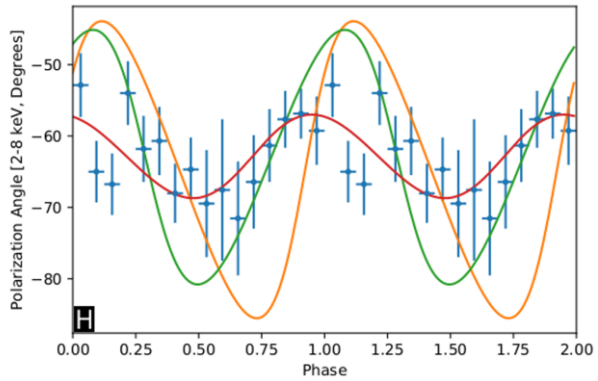
Magnetars

R. Taverna, R. Turolla, F. Muleri, J. Heyl, S. Zane, L. Baldini et al., 2022; S. Zane, R. Taverna, D. G. Caniulef, F. Muleri, R. Turolla, J. Heyl, K. Uchiyama, M. Ng, T. Tamagawa and I. Caiazzo et al., 2023



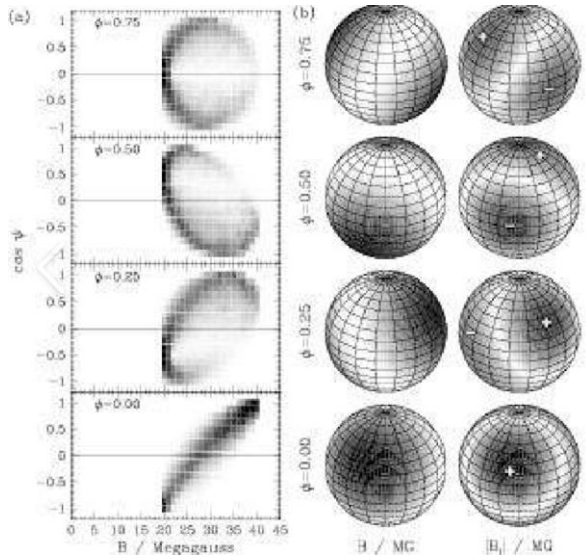


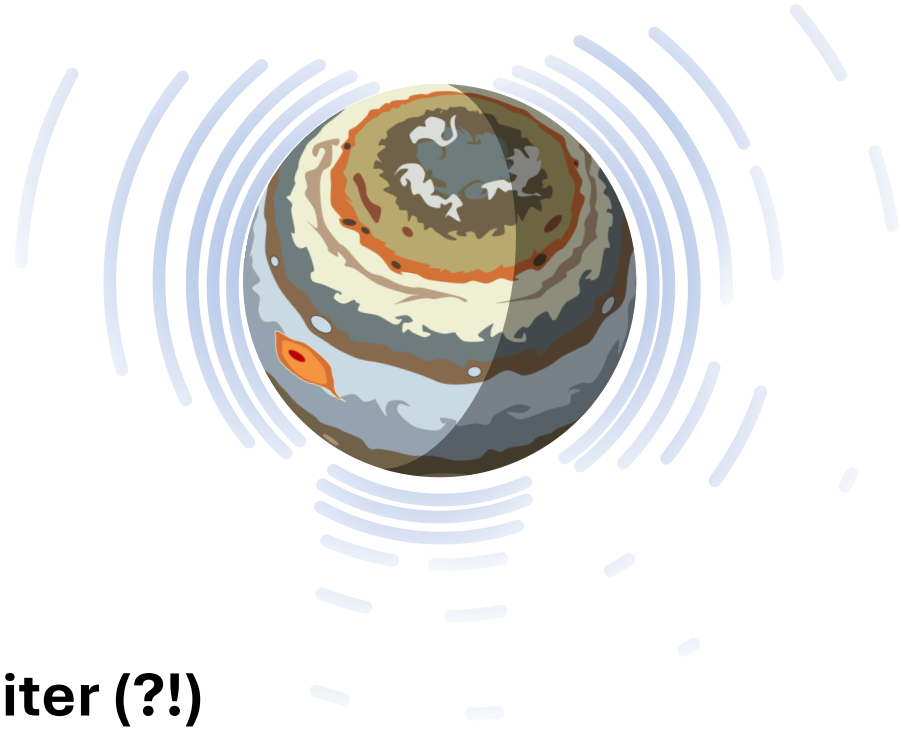




- Very bright sources, allowing to obtain structural information
- Significant astrophysical background

What's Next?





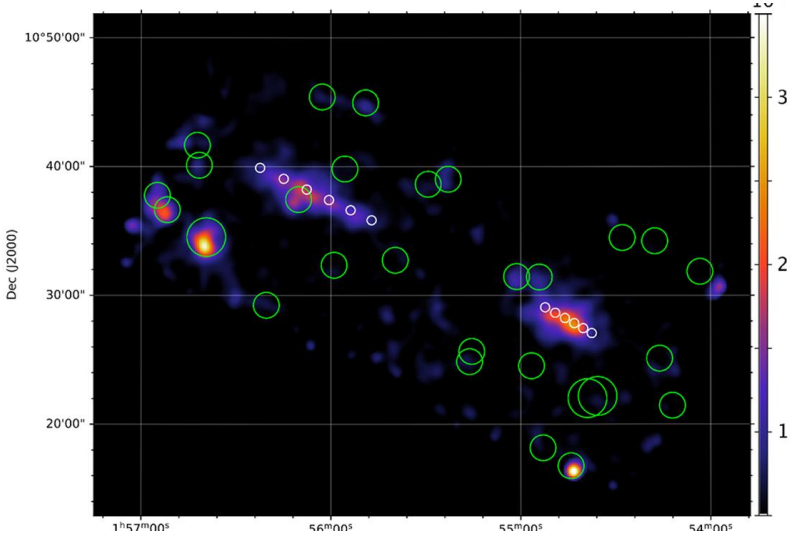
Magnetic White Dwarfs

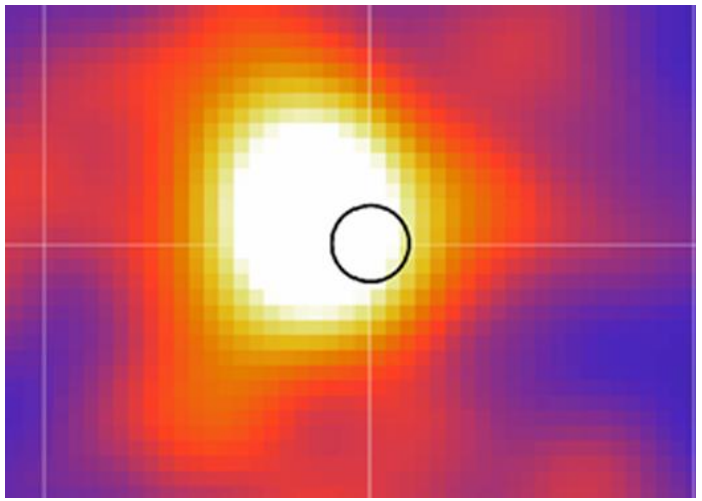
- ❑ Lower systematic uncertainty
- ❑ Very different magnetic field and internal production

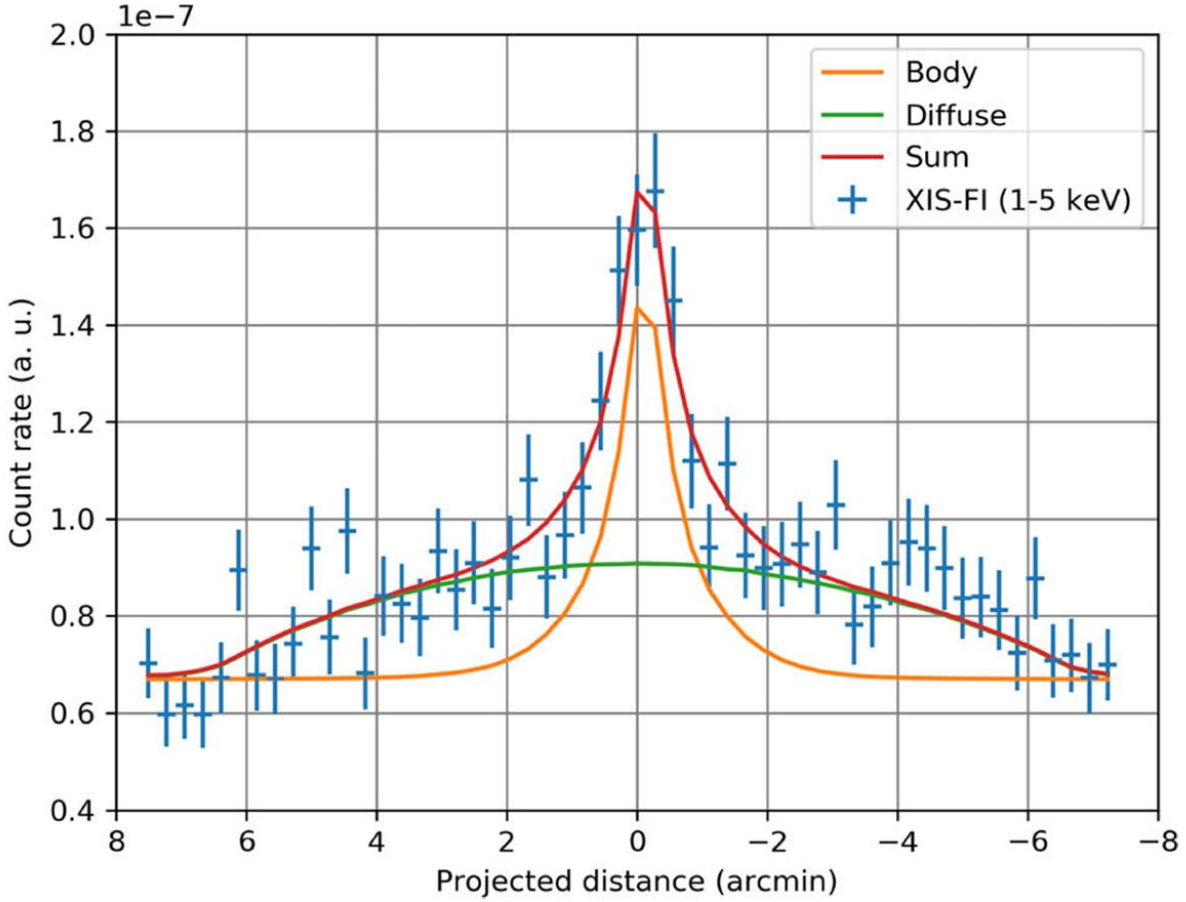
- ❑ **Jupiter (?!)**
- ❑ Not about ALP this time
- ❑ X-ray diffuse emission observed
- ❑ Need to predict the polarization property

Suzaku X-ray Excess around Jupiter

Yuichiro Ezoe et al., 1001.0800;
Masaki Numazawa et al.1906.06123

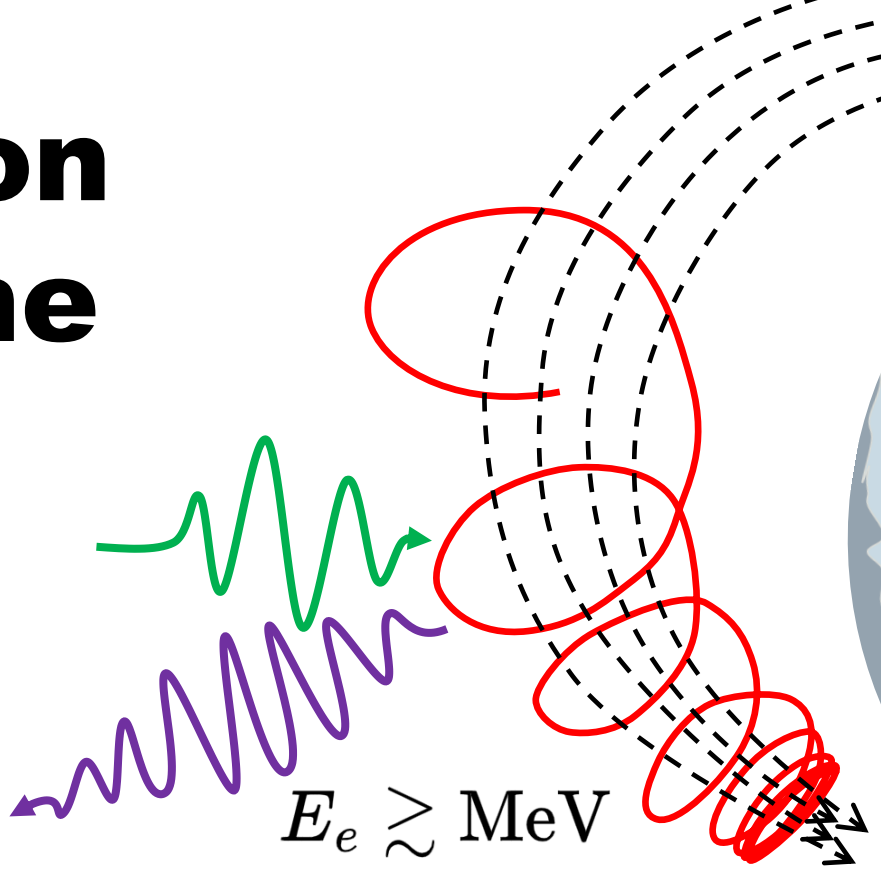


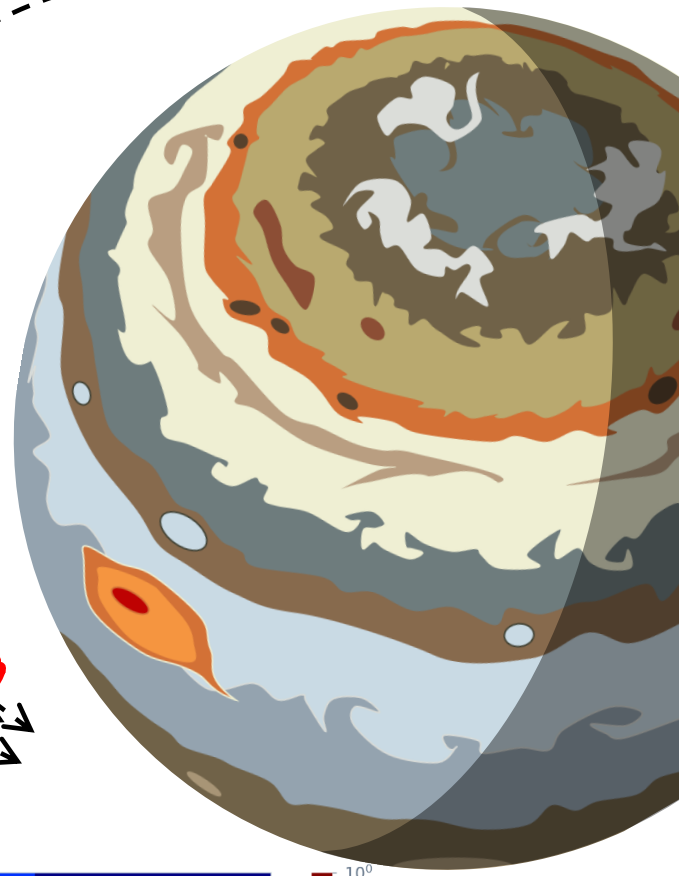




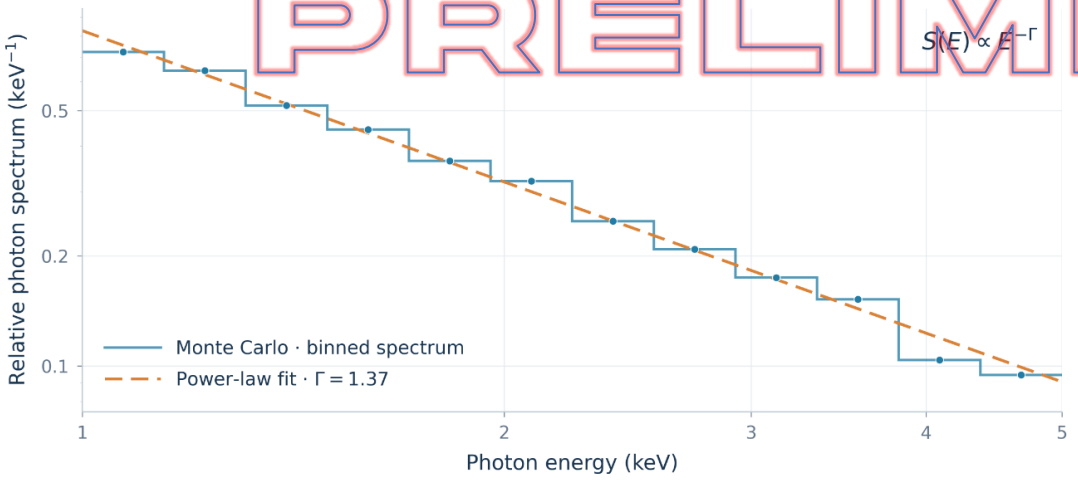
Inverse Compton Scattering in the Radiation Belt

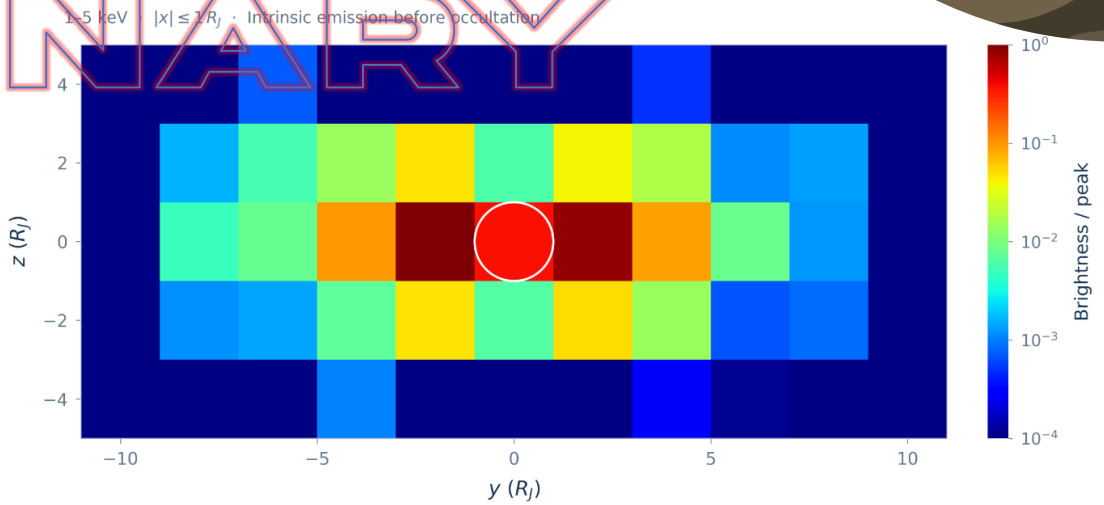
- Could be useful to constrain anomalous high-energy injections (by DM) J. Fan, LFL 2207.13709



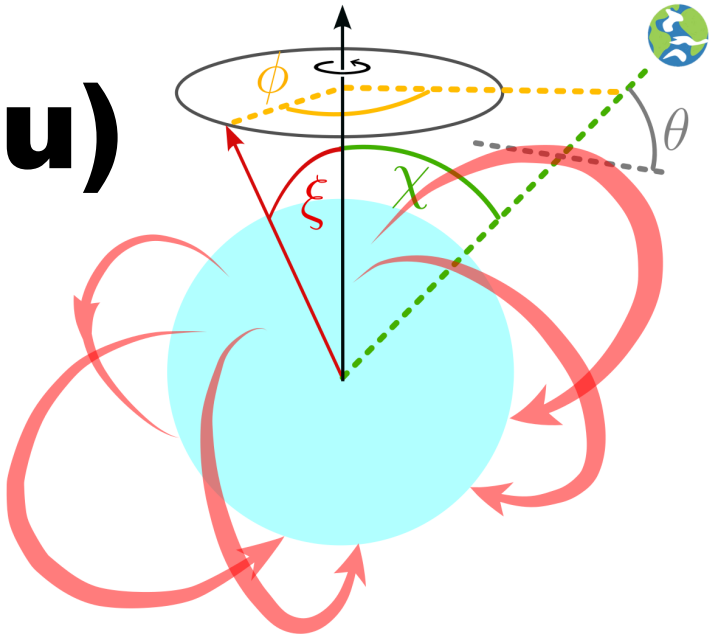


PRELIMINARY

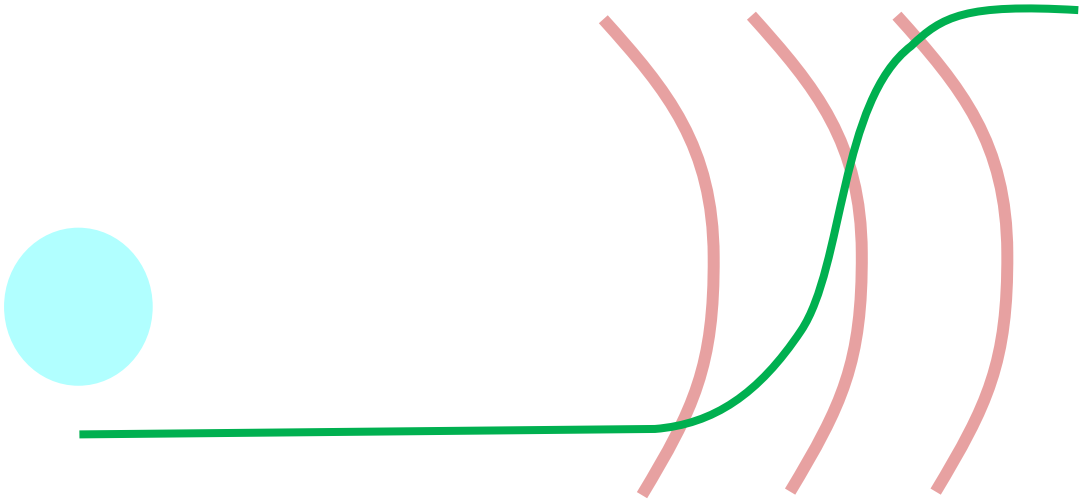




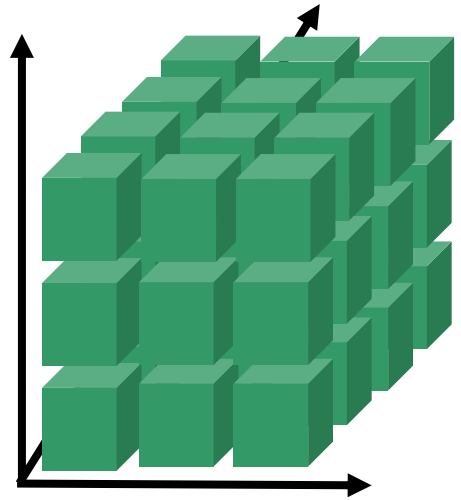
Summary (and Thank You)



- Polarization and pulse structures naturally arises with moderate axial symmetry breaking



- Energy-independent & insensitive to detailed corrections



- Analyzing 3/4D info (energy, polarization, time) helps discriminate models